Islombek MAMATOV

DESIGN AND FABRICATION OF UNIDIRECTIONAL SURFACE ACOUSTIC WAVE SENSORS

M.S.
2015

FATİH UNIVERSITY

The Graduate School of Sciences and Engineering

Master of Science in
Electrical and Electronics Engineering

DESIGN AND FABRICATION OF UNIDIRECTIONAL SURFACE ACOUSTIC WAVE SENSORS

by

Islombek MAMATOV

July 2015

DESIGN AND FABRICATION OF UNIDIRECTIONAL SURFACE ACOUSTIC WAVE SENSORS

by

Islombek MAMATOV

A thesis submitted to

the Graduate School of Sciences and Engineering

of

Fatih University

in partial fulfillment of the requirements for the degree of

Master of Science

in

Electrical and Electronics Engineering

July 2015
Istanbul, Turkey

APPROVAL PAGE

This is to certify that I have read this thesis written by Islombek MAMATOV and that in my opinion it is fully adequate, in scope and quality, as a thesis for the degree of Master of Science in Electrical and Electronics Engineering.

_____
Asst. Prof. Hüseyin SAĞKOL
Thesis Supervisor

I certify that this thesis satisfies all the requirements as a thesis for the degree of Master of Science in Electrical and Electronics Engineering.

_____
Prof. Onur TOKER
Head of Department

Examining Committee Members

Asst. Prof. Hüseyin SAĞKOL _____

Assoc.Prof. Erdal KORKMAZ _____

Asst.Prof. Alper ŞİSMAN _____

It is approved that this thesis has been written in compliance with the formatting rules laid down by the Graduate School of Sciences and Engineering.

_____
Prof. Nurullah ARSLAN
Director

July 2015

DESIGN AND FABRICATION OF UNIDIRECTIONAL SURFACE ACOUSTIC WAVE SENSORS

Islombek MAMATOV

M.S. Thesis – Electrical and Electronics Engineering
July 2015

Thesis Supervisor: Asst. Prof. Hüseyin SAĞKOL

ABSTRACT

Surface-wave devices are beginning to have an impact in radar, chemical, medical, bio-chemical, biomedical and communications systems. All these areas of application are reviewed with particular reference to code generation and matched filtering (pulse compression) for high-performance radars, correlation systems for simple radars, synthetic-clutter generation for clutter-reference radars, compressive receivers, processors for fusing and filter for acquisition of synchronization in communication systems, measuring bio-medical and bio-chemical datas.

Most of applications needs unidirectional (UDT) surface acoustic wave (SAW) devices in order not to cause reflection and interference in output signals. Bunch of parametric studies were made using ANSYS and COMSOL simulation software's. Parametric analysis like: interdigital transducers (IDT) height, IDT thickness, substrate material type, substrate material thickness, delay between receiver and transmitter IDT arrays, distance between IDT electrodes, horizontal distance between IDT electrode and substrate wall and etc.

After receiving simulation results, the results were compared to theoretical concept. When theoretical and simulation results were confirmed, fabrication steps and the process was proposed and then fabricated. Further works can be considered in integrating UDT IDT SAW devices with CMOS to be able to use in biomedical applications.

Keywords: Surface acoustic wave, uniderctional, interdigital tranducers, electrode, array

YÜZEY AKUSTIK DALGA FILTRELERI

Islombek MAMATOV

Yüksek Lisans Tezi – Elektrik ve Elektronik Mühendisliği
Haziran 2015

Tez Danışmanı: Asst. Prof. Dr. Hüseyin SAĞKOL

ÖZ

Yüzey dalgası cihazlar radar, kimyasal, tıbbi, biyo-kimyasal, biyomedikal ve iletişim sistemlerinde bir etkiye sahip olmaya başlıyor. Füzyon ve filtre için yüksek performanslı radarlar, korelasyon, basit radarları için sistemlerin, dağınıklığı referans radarlar için sentetik dağınıklığı nesil, basınç alıcıları, işlemciler için kod üretimi için özel referans ve uyumlu filtreleme (darbe sıkıştırma) ile gözden geçirilir iletişim sistemlerinde senkronizasyon edinimi, biyo-medikal ve biyo-kimyasal veriler ölçmekiçin uygulanabilir.

Uygulamaların çoğu çıkış sinyalleri yansıma ve parazite neden olmamak için tek yönlü (UDT) yüzey akustik dalga (SAW) cihazları ihtiyacı var. Parametrik çalışmalar ANSYS ve COMSOL simülasyon yazılımlarını kullanılarak yapılmıştır. Interdijital dönüştürücüler (IDT) yüksekliği, IDT kalınlığı, alt tabaka malzemesi türü, alt tabaka malzemesi kalınlığı, alıcı ve verici IDT diziler arasında gecikme, IDT elektrotlar arasındaki mesafe, IDT elektrot ve yüzey duvarı vb arasındaki yatay mesafe: gibi parametrik analizler yapılmıştır

Simülasyon sonuçları aldıktan sonra, sonuçlar teorik kavramla karşılaştırıldı. Teorik ve simülasyon sonuçları teyit edildiğinde, üretim aşamaları ve süreci önerİLdi ve sonra üretildi. Ayrıca, ilerki çalışmalar biyomedikal uygulamalarda kullanmı için CMOS UDT IDT SAW cihazları iel entegre olarbilmesi üzerinde olabilir.

Anahtar Kelimeler:. Yüzey akustik dalga, tek yönlü, interdijital dönüştürücüler, elektrot,dizi

To my parents
For their endless love and support

ACKNOWLEDGEMENT

I sincerely trace my gratitude to Asst. Prof. Alper ŞİŞMAN and Asst. Prof. Hüseyin SAĞKOL for their honest guidance in my research activities. There generous attitude permitted me to learn a lot both theoretically and practically about my fields of interest.

Further, I would like to acknowledge all other professors of Fatih University for helping me in my graduate education by providing me solid theoretical backgrounds. .

I am absolutely grateful to my parents for their support in all means and their patience. I would like to also thank my brothers, friends and colleagues that embellished my degree with excitations and lots of recreative activities. I also thank my wife for supporting me and showing patience during my research and education years.

I would like to express my specific gratitude to my teammates from “FC KAGANAT” which gave me lots of sportive activity and joy and became champions on a league tournament organized in Istanbul in 2014-2015 by Kyrgyzstan students.

TABLE OF CONTENTS

LIST OF TABLES

TABLE

LIST OF FIGURES

FIGURE

LIST OF SYMBOLS AND ABBREVIATIONS

SYMBOL/ABBREVIATION

AC	Alternating current
c	Speed of sound
CMOS	Complementary metal oxide semiconductor
dB	Decibels
DC	Direct current
f	Frequency
FSI	Fluid structure interface
G_o	Characteristic admittance
GHz	Gigahertz
IDT	Interdigital transducer
IF	Infrared frequency
k	Wavenumber
LSAW	Flawed surface acoustic wave
MHz	Megahertz
RF	Radio frequency
RX	Receiver
SAW	Surface acoustic wave
SSBWT	surface-skimming mass wave
STW	Surface transverse wave
TX	Transmitter
UDT	Unidirectional transducer
UV	Ultraviolet
Υ_s,	Image parameter
Δ	Gradient
λ	Wavelength
ρ	Density

CHAPTER 1

INTRODUCTION

1.1 BASIC BACKGROUND

Electronic signal processing by method for the specific control of surface acoustic waves on piezoelectric substrates was started in 1965 with the creation of the thin-film interdigital transducer (IDT) by White and Voltmer at the University of California, at Berkeley. Their thought was misleadingly straightforward, however shrewd. The method was to manufacture metal Thin-film IDTs on the surface of a compatible piezoelectric substrate that would be acting as electrical input and Output ports. Use of a fitting AC,DC or even AC+DC voltage jolt to the input transducer propelled and controlled by a surface acoustic wave (SAW). The receiver transducer identified the occurrence surface acoustic wave and convert it back to a suitably filtered electrical one. This surface acoustic wave sort was a Rayleigh wave, with movement bound to around one acoustic wavelength under the free surface of the piezoelectric.

The electronics industry immediately perceived that such SAW signal processing could promptly be applied to the outline of simple electrical filters working at chose frequencies in the extent from about l0MHz to 1GHz. Regardless of this, it was sooner or later before it was admired that an IDT could be considered to represent to a sampled structure to which advanced digital data sampling ideas could be applied.

The former moderate development situation has changed more drastically lately. With the revelation and usage of different sorts of surface acoustic waves (frequently alluded to as pseudo-SAW), made conceivable by the disclosure of new piezoelectric substrates and for crystal cuts. To date, these incorporate the flawed surface acoustic wave (LSAW), the surface-skimming mass wave (SSBWT) and the surface transverse wave (STW). The usage of LSAW strategies has been especially noteworthy. As it has

opened up the passage to the utilization of low-loss {e.g..1 to 3dB) RF Front-end filters and antenna Duplexers for portable/remote transceivers.

Alongside the Rayleigh wave, these three extra previously stated wave sorts are likewise ordinarily alluded to as surface acoustic waves. This widely inclusive classification has additionally been received in the title of this book. For illumination in the content. Notwithstanding, the particular wave sort will be distinguished as needed.

1.2 BENEFITS OF SURFACE ACOUSTIC WAVE DEVICES

As noted by Hartmann in a 1985 audit paper on the frameworks effect of SAW-then an entirely Rayleigh wave-innovation. Numerous such gadgets and frameworks showed a few phenomenal components when contrasted with contending advancements of that time. A large portion of these early components is still substantial, as included here:

Surface acoustic wave devices can generally be intended to give very unpredictable signal processing capacities inside of a solitary bundle that contains just a solitary piezoelectric substrate with superimposed meager film input and output interdigital transducers. In this way, for instance, bandpass filters with extraordinary reaction qualities can now be routinely intended to accomplish reactions that would require a few hundred inductors and capacitors in traditional LC filter designs.

They can be mass produced utilizing semiconductor microfabrication procedures. Thus, they can be made to be cost-aggressive in mass-volume applications, with a few items offering for less than $1.00.

They can have extraordinary reproducibility in performance from gadget to gadget. This is particularly attractive in the design of radio frequency {RF} and IF channels for cell telephones, narrowband high-Q resonators, and also for channelized beneficiaries for ghastly examinations or different frameworks obliging exactness filtering.

As they can be actualized in little, rough, light and power-effecient modules, they are new standard segments in portable, remote, and space-borne communication systems.

Surface acoustic wave filters can be made to work in high-harmonic modes. A few devices for the 2-GHz band are presently being manufactured in this way so as to meet requesting lithographic resistances and imperatives. One sample is for 2.433-GHz timing-extraction filters in optical-communication links, where a long haul Phase stability of 20° is needed more than a 20-year period [1].

1.3 LITERATURE SURVEY

On the off chance that the objective is to excite a solitary acoustic mode, on the top of a subsrtate the transducer is placed, and by utilizing an interdigital transducer (IDT) structure an acoustic mode waves can be generated by selectively exciting. For producing surface acoustic waves (SAW) on top of a piezoelectric substrates , utilization as simple filters IDTs were initially produced. Since than, innumerable number of sensors have been created utilizing surface acoustic waves, including compound sensors biosensors, and mass sensors. Fingers ot thin cathodes, or an metal thin film interdigital transducer, organized in a substituting grouping as outlined in the accompanying figure [7] [2], [3].

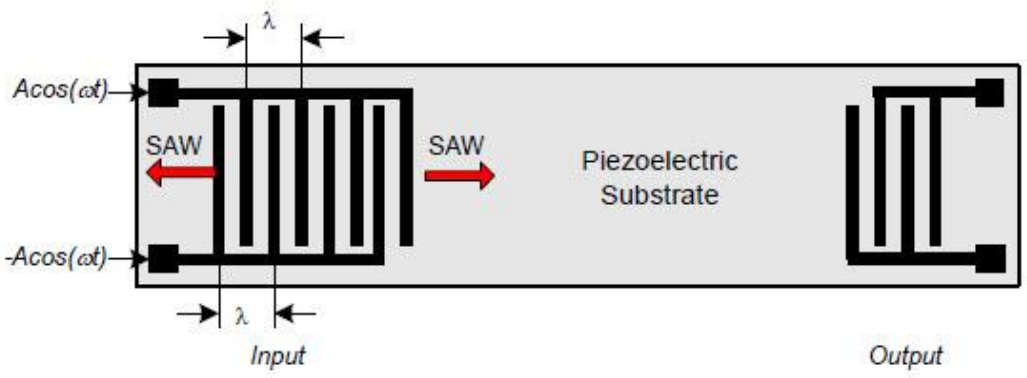

Figure 1.1 Schematic of a typical interdigital acoustic transducer.

Metal thin film inter digital trasnducers regularly placed one half of acousticc wavelenght λ, with respect to neighboring electodes. To create a bi-directional surface acoustic wave traviling in the piezoelectric substrate each legs of the IDT groups are energized with different polarities signals of same amplitude. the transducer starts to act more like a filter that selectively excites a single acoustic mode, as the quantity of electrode combines, or fingers, is expanded, [7]

In this work, our goal is to generate unidirectional acoustic waves, by changing the spacing between the neighboring electrodes. This phenomenon is achieved when you make the spacing between the neighboring electrodes in the IDT one four of the wavelength of the desired acoustic mode, λ that is λ/4. After, to observe the directionality of surface acoustic wave by changing several parameters like substrate type, substrate thickness, substrate length, material type of electrode, weight of electrode and a length of electrode and e.t.c. At the end optimal device is going to be fabricated and tested for further applications like bio-sensors. [7] [4]

CHAPTER 2

A DESCRIPTIVE STUDY OF SURFACE ACOUSTIC WAVES AND PIEZOELECTRIC MATERIALS

A detailed study t of surface acoustic waves and piezoelectric materials will be provided in order to understand the behavior of acoustic wave to make them unidirectional. Hence, the goal is to simulate, design and fabricate best performance unidirectional surface acoustic wave sensor.

2.1 SURFACE ACOUSTIC WAVES AND THEIR GENERATION

Mass-spring system in which relocation of a flexible medium acts as a conveyed a solitary component brings about the spread of an aggravation all through the solid. In relation to one inside to the solid a molecule at a free surface is unique. Meaning the particle compelled by contiguous particles from one and only side. Accordingly, aggravations at a surface can act to some degree uniquely in contrast to those in the inside of a solid. Truth be told, such limit contemplations offer ascent to interesting methods of spread that can just exist at the free surface of a solid. Before considering such alleged surface waves. It is informational to inspect plane waves that proliferate a long way from any annoying limits.

Pretty much as a mass/spring system sways because of the interchange of an inertial power connected with the mass with a restoring power from the spring, a flexible wave emerges from the transaction of circulating flexible and inertial powers. Differential equation can be used to portray the spring/mass framework reaction, where mass time and displacement included. However the motion of a wave in the strong is

the kind of more mind boggling. Molecule relocation in the strong is a capacity both of position and time, such as one-dimensional oscillating spring, and the mathematical statement of movement must be a restricted description. [6]

Relying on the boundaries of the strong and its properties the waves can propagate in a solid [5]. In Figure 2.1 it can be seen that waves are propagating systematically in an unbounded medium, solitary plane boundary in a semi-infinite medium, and two plane limits has a solid plate. Definitions, investigations and phrasing that follow in this part are utilized to focus the phase velocities of the waves especially solids. And the way of these wave motions [6]

The flexible wave's representations in solids, movements of gatherings of particles are portrayed in these cross-sectional perspectives of plane flexible waves spreading to one side. Horizontal and vertical displacements overstated for clarity. Beneath every portrayal ordinary wave speeds, Vp are demonstrated.

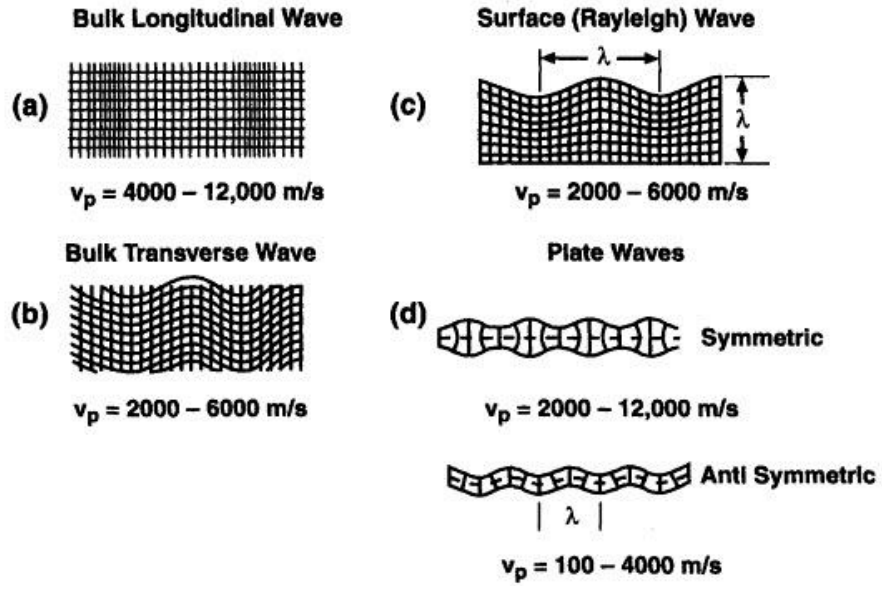

Figure 2.1 (a) in unbounded solid compressional wave. (b) In unbounded solid shear wave (bulk transverse). (c) In semi-unbounded solid Surface acoustic wave, where beneath the surface to a depth wave movement stretches out of around one wavelength. (d) Plates Waves in thin solid. [6]

2.1.1 Strain, Stress and Displacement

It puts the solid strong under stress application of force. Inside of the solid stress brings about the strain: particles or atoms of where the strong is formed are dislodged from its strained areas. At the point where a strong is twisted, every molecule from its unique position and the relocation is spoken to by a displacement vector u (x, y, z, t}. The displacement commonly has parts, those shift constantly in the solid, from point to point in the x, y and z directions. If this is the wave engendering x direction a plane wave creates relocations that shift agreeably toward. Since, deduction can be made such as:

$$u(x,y,z,t) = (u_1 x + u_2 y + u_3 z)e^{j(wt-kx)} \tag{2.1}$$

Where u_1, u_2, and u_3 in the x, y and z directions speak to atom displacement. Individually: in their separate directions x, y, and z are unit vectors: w is the angular frequency of the wave, planes opposite to the engendering direction for a plane wave that forms of steady displacement. Also, we can recall elementary equations like: [6]

$$w = 2\pi f \tag{2.2}$$

$$k = \frac{2\pi}{\lambda} \tag{2.3}$$

$$j = \sqrt{-1} \tag{2.4}$$

Where f is frequency ,k is wavenumber and λ is wavelength.

Motion is killed to result a value related just to *local deformation* of the solid, since straightforward interpretation of the solid is not area of interest. Δu, is a parameter that states for a displacement gradient, where the slope of a vector field Δu is a second-rank tensor, indicated by a 3 by 3 matrix given below as:

$$\Delta u = \begin{pmatrix} \partial u_1/\partial x & \partial u_1/\partial y & \partial u_1/\partial z \\ \partial u_2/\partial x & \partial u_2/\partial y & \partial u_2/\partial z \\ \partial u_3/\partial x & \partial u_3/\partial y & \partial u_3/\partial z \end{pmatrix} \tag{2.5}$$

The displacement gradient speaks to changes in interparticle distance and additionally local rotations created by the displacement [5].

We have to review our basic skill from physics and state that, strain is force applied a material like solid. However, strain is the dimensional ratio length of stressed material to its unstressed length. In figure 2.2 we can see an illustration of plane wave propagation in solid.

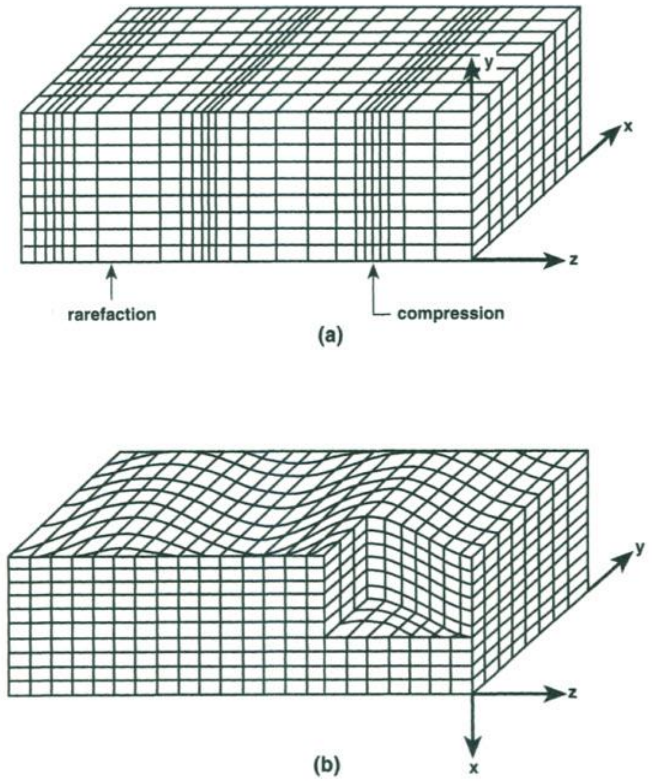

Figure 2.2 an illustration of plane wave propagation in solid (a) compressional (b) shear waves.

As we stated before strain is the adjustment long per unstrained unit length in the solid as an aftereffect of connected stress and can be evaluated for any direction, in the solid from the strain tensor. As a result strain matrix ***S*** with elements can be written as:

$$s_{ij} = \tfrac{1}{2}(\partial u_i / \partial x_j + \partial u_j / \partial x_i) \qquad (2.6)$$

To speak to totally the condition of stress at every point in a solid obliges utilization of a stress tensor, T. Every component at the stress tensor, T_{ij}, speaks to the i^{th} part of force per zone following up on the j^{th} face of a microscopic volume component. T permits the determination of the stress in any direction on any plane inside of the solid. The stress vector following up on a plane with a typical segment as determined by the direction cosines (l_1, l_2, l_3) is given by $T_{ij}l_j$. [6].

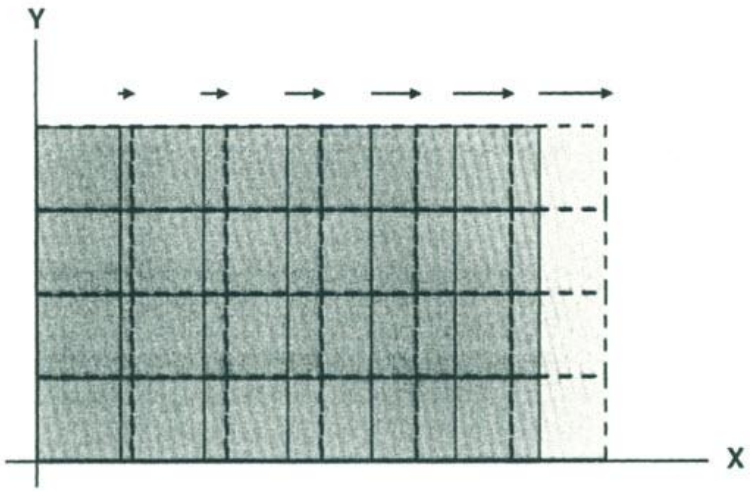

Figure 2.3 Bar under uniaxial strain.

2.1.2 Equation of Motion

Meaning of stress and strain licenses induction of the mathematical statement of motion for elastic deformations of a solid, specifically wave motion. Figure 2.4 demonstrates an essential volume of an elastic solid.

The stress that applies compels in the x direction of every face are demonstrated, with the suspicion that stress has just changed a small amount, ΔT_i over the essential lengths Δx, Δy, Δz. The force applied on every face is the result of the stress segment showed times the region over which the anxiety demonstrations The summation of the greater part of the x-coordinated strengths following up on the cube is therefore:

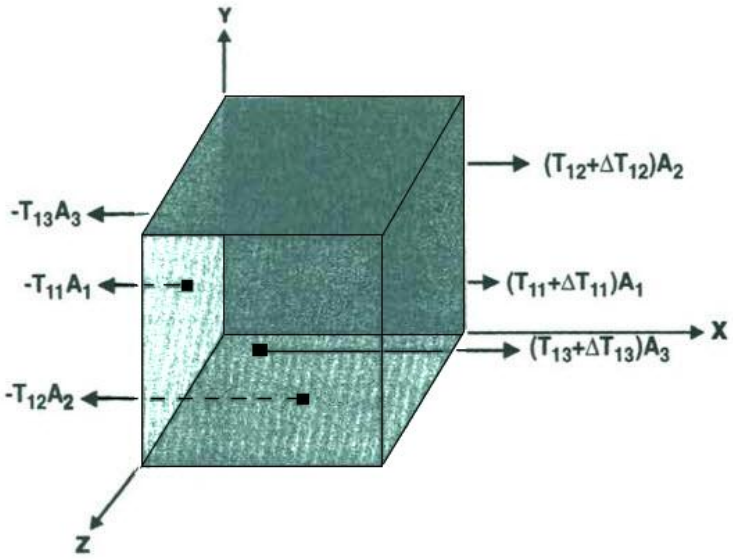

Figure 2.4 Elemental volume of an elastic solid, showing the forces exerted on each face.

$$F_1 = [(T_{11} + \Delta T_{11})A_1 - T_{11}A_{11}] + [(T_{12} + \Delta T_{12})A_2 - T_{12}A_{12}] + [(T_{13} + \Delta T_{13})A_{13} - T_{13}A_3] \quad (2.7)$$

Also, the area of face with normal component in x_i direction is

$$A_i = \sum_{jk} \delta^{ijk} \Delta x^j \Delta x^k (i \neq j \neq k) \quad (2.8)$$

Where its acceleration and Newton's laws respectively are

$$\ddot{u}_i \equiv \partial^2 u_i / \partial t^2 \quad (2.9)$$

$$F = m\ddot{u} \quad (2.10)$$

The mass of elemental volume can be written as $\rho \Delta x \Delta y \Delta z$ where ρ denotes density (mass/volume) of the solid. Since, from the equations above equation 2.7 and Newton's law we can induce the following mathematical statement

$$\Delta T_{11}\Delta y\Delta z + \Delta T_{12}\Delta x\Delta z + \Delta T_{13}\Delta x\Delta y = \rho \Delta x\Delta y\Delta z \frac{\partial^2 u_1}{\partial t^2} \quad (2.11)$$

If we divide the equation above by $\Delta x \Delta y \Delta z$,we can get one-dimensional partial differential equation and finally equation of motion can be generalized as

$$\sum_{j=1}^{3} \frac{\partial T_{ij}}{\partial x_j} = \rho \frac{\partial^2 u_i}{\partial t^2} \qquad \textit{Equation of motion} \qquad (2.12)$$

The principle that relates stress to strain is known as consecutive relation, and can be generalized to three-dimensional, non-piezoelectric solid

$$T_{ij} = \sum_{k,l=1}^{3} c_{ijkl} S_{kl} \qquad \textit{Elastic Constitutive Relation} \qquad (2.13)$$

In which the c_{ijkl} called elastic stiffness consistent, serve as "tiny spring constants" in depicting what strain results from a given stress. The elastic constants totally describe the elastic conduct of a solid in the small deformation limit [6].

2.1.3 Wave Equation

From the equation of motion (Equation 2.12) and the elastic constitutive equation (Equation 2.13) we can simply drive new equation, wave equation. Which depicts propagation of plane acoustic wave in non piezoelectric solid. Differentiating equation 2.13 with respect to x_j gives

$$\sum_{j=1}^{3} \frac{\partial T_{ij}}{\partial x_j} = \sum_{j,k,l}^{3} c_{ijkl} \frac{\partial^2 u_k}{\partial x_j \partial x_l} \qquad (2.15)$$

Equating right hand sides of Equations 2.12 and 2.15 results in wave equation for non-piezoelectric elastic, solid.

$$\rho \frac{\partial^2 u_i}{\partial t^2} = \sum_{j,k,l=1}^{3} c_{ijkl} \frac{\partial^2 u_k}{\partial x_j \partial x_l} \qquad \textit{Non-piezoelectric Wave Equation} \qquad (2.16)$$

It ought to be noticed that Equation 2.16 speaks to an arrangement of three wave mathematical statements (j=1,2,3) with the addition over the actuates $j, k\ and\ l$ for the molecule displacement u_1, u_2, and u_3, and the propogation of a wave alludes to the heading of molecule relocation. The answer for Equation 2.1 comprises of three wave types propagating such as: a quasi-compressional wave, whose direction of propagation is the main polarization. What's more, whose important polarization is opposite to the propagation direction which are known as quasi-shear waves, showed in Figure 2.2. Comparison 2.16 kind of forcing. In any case, in specific examples it diminishes to an exceptionally basic arrangement of comparisons.

$$u_i(x,t) = u_{i0}e^{j(wt-kx)} \tag{2.17}$$

Speaking to wave +x direction polarization: u0 is the amplitude andu_j, is the displacement in the i^{th} direction. Hence u_1 lies along the direction of propagation. the arrangement $u_1(x,t)$ speaks to a wave polarizing in a x pivot , where u_2 and u_3 speak to two shear waves traveling along +x, as demonstrated in Figure 2.2(b). By noting that:

$$\rho \frac{\partial^2 u_1}{\partial t^2} = c_{11} \frac{\partial^2 u_1}{\partial x^2} \tag{2.18}$$

$$\rho \frac{\partial^2 u_3}{\partial t^2} = c_{44} \frac{\partial^2 u_3}{\partial x^2} \tag{2.19}$$

$$\rho \frac{\partial^2 u_2}{\partial t^2} = c_{44} \frac{\partial^2 u_2}{\partial x^2} \tag{2.20}$$

$$\partial^2 u_i / \partial t^2 = -\omega^2 u_i \tag{2.21}$$

$$\partial^2 u_i / \partial x^2 = -k^2 u_i \tag{2.22}$$

And by substituting Equation 2.15 into Equations 2.18 and 2.19 above, *dispersion relation* equation can be derived for the compressional wave:

$$\rho\omega^2 = c_{11}k^2 \qquad \textit{Dispersion Curve} \tag{2.23}$$

2.2 PIEZOELECTRICITY

The coupling between of strain and electrical polarization that happens in numerous crystals gives an intends to creating acoustic waves electrically. At the point when the structure of a crystal does not have a focal point of reversal symmetry, the use of strain changes the conveyance of charge on the particles and bonds embodying the crystal in such a way, to the point that a net,macroscopic, naturally visible, electrical polarization of the crystal results. As seen in figure 2.5.

The creation of electric displacement by the use of a mechanical stress is the direct piezoelectric impact. When an electric field is connected to a piezoelectric material the opposite piezoelectric impact brings about the generation of a strain. The connection between stress and strain,. is demonstrated by the expression "Elasticity," by Equation 2.1. Numbers in square brackets demonstrate the positions of the crystal property tensors: the piezoelectric coefficients are 3rd-rank tensors. Furthermore, the elastic stiffnesses are 4^{th}-rank tensors. Numbers in parenthesis recognize lst-rank tensors (areas. for example, electric field and electric displacement) also, 2nd-rank tensors (stress and strain).

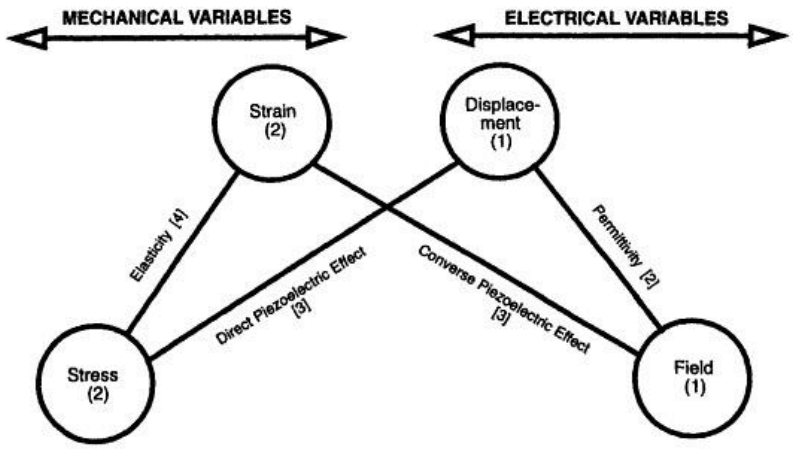

Figure 2.5 Relations among mechanical and electrical variables for a crystals.

The coupling between electric field and strain can be represented by a fitting adjustment to the elastic constitutive relation (Equation 2.13).

$$T_1 = c_{ij}^{E} s_j - e_{ij} E_j \tag{2.24}$$

$$D_i = \in_{ij}^{s} E_j + e_{ij} S_j \tag{2.25}$$

The piezoelectric stress constants which is e_{ij} are, having units of$(\text{charge}/\text{length})^2$ where, D_i are the electrical displacement parts E_i are the electric field segments, and ϵ_{ij} are the permittivity constants. Mathematical statements in the above, known as the piezoelectric constitutive relations, totally portray the interchange of strain, stress, and electric field in a piezoelectric materails [6].

2.2.1 The Wave Equation for Infinite Piezoelectric Materails

It is a basic matter to determine the wave Equation for piezoelectric media from the piezoelectric constitutive relations. Mathematical statement of the piezoelectric wave is ordinarily composed as far as the displacementu_i, combined with an electrical potential, ϕ, instead of combined with the electric field partsE_i. Taking note of that,

$$E_k = -\partial\phi/\partial x_k \tag{2.26}$$

we can compose Equation 2.24 as

$$T_{ij} = \sum_{k,l=1}^{3} c_{ijkl} \frac{\partial u_l}{\partial x_k} + \sum_{k=1}^{3} e_{ijkl} \frac{\partial \phi}{\partial x_k} \tag{2.27}$$

Application of motion to the Equation 2.24 will give

$$\sum_{j,k,l=1}^{3} c_{ijkl} \frac{\partial^2 u_l}{\partial x_k \partial x_j} + \sum_{j,k=1}^{3} e_{ijk} \frac{\partial^2 \phi}{\partial x_k \partial x_j} = \rho \frac{\partial^2 u_i}{\partial t^2} \tag{2.28}$$

In the event that Equation 2.28 is contrasted and the wave mathematical statement in non-piezoelectric media (Equation 2.16}, the vicinity of an extra term

including the electrical potential ϕ is evident. This term may be assumed as a source term in charge of the ***generation of an acoustic wave*** from an applied time-changing electrical potential. Alternately, the wave relocations create an accompanying electrical potential through where the piezoelectric wave may be electrically distinguished

CHAPTER 3

UNIDIRECTIONAL SURFACE ACOUSTIC WAVE SENSORS

In this chapter, the conventional surface acoustic wave devices that generate bi-directional waves will be introduced. How they work, types of sensors, and their applications also will be talked. After, generation of unidirectional (UDT) inter digital (IDT) type sensors and mathematical approach to 3-port IDT modeling will be tried to be explained.

3.1 SURFACE ACOUSTIC WAVE SENSORS

3.1.1 Bi-directional SAW

SAW has been successfully employed in a number of signal-processing devices, such as RF filters, IF filters, duplexers and other SAW devices for recent digital mobile communications, chemicals and bio-sensors.

The stress-free limit forced from the surface of a crystal offers ascend to an exceptional acoustic mode whose proliferation is confined to the surface and is along these lines known as a surface acoustic wave (SAW). In 1887 Lord Rayleigh found this method of propagation in which acoustic vitality is limited close to the surface of an isotropic solid. This mode, now known as the Rayleigh wave. The utility of Rayleigh waves in sensor applications is likewise because of the surface segment of vitality, permitting them to be energized by surface cathodes in piezoelectric materials furthermore making the wave amazingly delicate in surface irritations

.

The saw sensors are passive elements (they do need power supply) and can be accessed wirelessly, enabling remote controlling in harsh environment. They work inthe frequency range of 10 MHz to several GHz. They have the rugged, compact structure, outstanding stability, high sensitivity, low cost, fast real time response, extremely small size

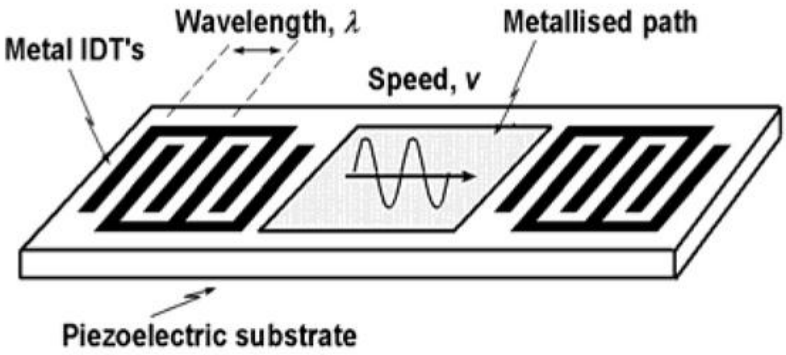

Figure 3.1 Basic structure of Surface acoustic wave sensor(SAW).

In the above figure the basic structure of bi-directional surface acoustic wave sensors is illustrated. In this illustration distance of the neighboring metal thin IDT electrodes are one half of the target acoustic wavelength λ. As we can see from figure there are two legs of metal thin IDT electrodes, upper and lower legs. Both upper and lower legs are energized with periodic signals of same amplitude but different polarities in order to create bi-directional surface acoustic waves. When someone increases the number of these metal thin IDT electrodes, the device should perform like filter , giving more selectivity to generate acoustic waves. [7]

The principal wave speaks to the acoustic field created by the transducer leg driven with the cos(ωt) signal and can be composed utilizing complex exponentials as

$$P_1 = Ae^{j\omega t}[e^{-jkx} + e^{jkx}] \quad (3.1)$$

Where A is the amplitude of the wave. The second wave is moved in time by a period of φ and in space by a separation of δ and can be composed

$$P_2 = Be^{j\omega t}[e^{-jkx}e^{-j\phi}e^{-jk\delta} + e^{jkx}e^{j\phi}e^{-jk\delta}] \quad (3.2)$$

Where *B* is the amplitude of the wave. By assumng that the two amplitudes are taken to be, A=B, one acquires [7]

$$P_{Total} = Ae^{j\omega t}[e^{-jkx}(1+e^{-j(\phi+k\delta)}) + e^{jkx}(1+e^{j(\phi-k\delta)})] \quad (3.3)$$

When φ=0 and δ=0, the amplitude of the pressure waves propagating in the +x and -x directions is 2A. In both directions, as expected [7]

$$P_{Total} = Ae^{j\omega t}[e^{-jkx}(1+e^{-j(0+k0)}) + e^{jkx}(1+e^{j(0-k0)})]$$

$$= Ae^{j\omega t}[e^{-jkx}(1+e^{0}) + e^{jkx}(1+e^{0})]$$

$$= Ae^{j\omega t}[2e^{-jkx} + 2e^{jkx}]$$

3.1.2 Unidirectional SAW (UDT IDT)

The non-piezoelectric film layer transducer speaks to the most effective technique for producing and recognizing surface waves on piezoelectric substrates. A run of the mill transducer structure comprises of an interdigital terminal n overlying on a substrate. Then again, it is no doubt understood that the acoustic-surface wave channel utilizing a customary interdigital transducer has an inborn property of the biphase transducer. That is, it has a bidirectionality loss of 6dB, and just 12 dB of triple-travel concealment is gotten in a perfectly matched filter.

It is conceivable to dispense with the bidirectionality misfortune totally by utilizing multiphase unidirectional transducers (u.d.t.). The multiphase commute evacuates the bidirectional symmetry and grants complete transformation from electrical signals to acoustic signals going in one direction. Therefore this structure has

no innate bidirectionality misfortune. This structure likewise stifles triple-travel impacts, in light of the fact that the yield transducer can retain all the episode acoustic force.

At the point when the phase is set to 90º, or π/2, the and distance is set to λ/4 ,according to Equation 3.3 deduction can be made on that the amplitude of the wave traveling in the -x-direction will be 0, and the amplitude of the wave going in the +x-direction will be 2A. By noting that $k = 2\pi/\lambda$; [7]

$$P_{Total} = Ae^{j\omega t}[e^{-jkx}(1+e^{-j(\frac{\pi}{2}+\frac{2\pi}{\lambda}\frac{\lambda}{4})}) + e^{jkx}(1+e^{j(\frac{\pi}{2}-\frac{2\pi}{\lambda}\frac{\lambda}{4})})]$$

$$= Ae^{j\omega t}[e^{-jkx}(1-1) + e^{jkx}(1+1)]$$

$$= Ae^{j\omega t}[0 + 2e^{jkx}]$$

and switched when pahes is set to -90 [7]

$$P_{Total} = Ae^{j\omega t}[e^{-jkx}(1+e^{-j(-\frac{\pi}{2}+\frac{2\pi}{\lambda}\frac{\lambda}{4})}) + e^{jkx}(1+e^{j(-\frac{\pi}{2}-\frac{2\pi}{\lambda}\frac{\lambda}{4})})]$$

$$= Ae^{j\omega t}[e^{-jkx}(1+1) + e^{jkx}(1-1)]$$

$$= Ae^{j\omega t}[2e^{-jkx} + 0]$$

Never less, there is a lot of methods to achieve unidirectionality. The method can be chosen according to the application. For example, someone can put gratings or acoustic wave absorbers on the edges of the piezoelectric susbtrates. However, this method is not optimal when there is Scholte waves that is result of solid and liquid interaction. For this Scholte wave needed applications unidirectional (UDT) interdigital (IDT) method that was also illustrated in figure 3.2 is best one and is subject of our interest. [7]

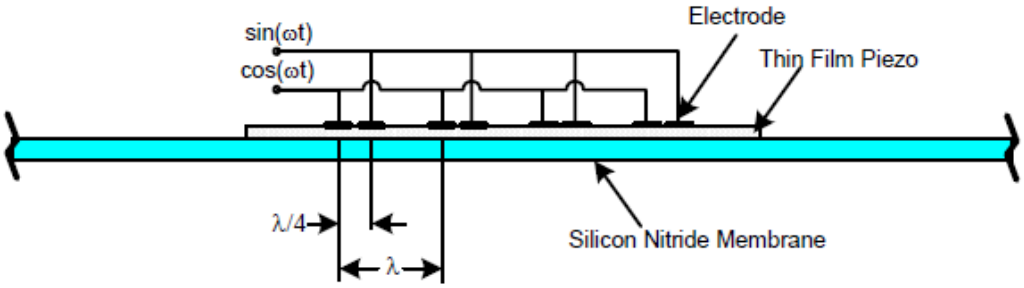

Figure 3.2 illustration of UDT IDT.

When designing UDT IDT every parameter is very important. Like electrode length, substrate length, electrode width, electrode height, substrate width, substrate height, finger pair number and etc. This parameter studies will be mentioned in further chapters.

3.2 MATHEMATICAL APPROACH TO MODEL 3-PORT SAW

3.2.1 Configuration of SAW sensor

We consider an ideal design of a three-IDT sort SAW sensor show in figure 3.2 The three-IDT type SAW sensor comprises of a few parts: transmitter (IDT-l), two receivers IDTs (IDT-2). For both of the receiver and the transmitter IDTs, we utilize a single electrode type IDT, which is generally utilized in light of its auxiliary straightforwardness

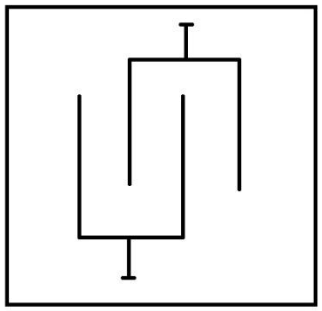

Figure 3.3 3-port SAW sensors.

3.2.2 Equivalent circuit model

So as to consider the acoustic-electric association created by IDT from the perspective of electric circuit hypothesis, different comparable circuit models of IDT have been produced Even however the proportionate circuit models proposed by Smith and his partners, 181 have been utilized generally to examine the recurrence reaction qualities of IDT. [8]

Figure 3.4 delineates the most recent proportional circuit model for one finger of IDT, where impedances Zl and Z2 are given in (3.4). In the four-port equal circuit model indicated in Fig 3.4, port-1 and port-2 compare to acoustic ports, while port-3 and port-4 are electric ports [8].

$$\begin{cases} Z_1 = \frac{R_0}{F_s} tanh(\frac{\gamma_s}{2}) \\ Z_2 = \frac{R_0}{F_s} cosech(\gamma_s) \end{cases} \tag{3.4}$$

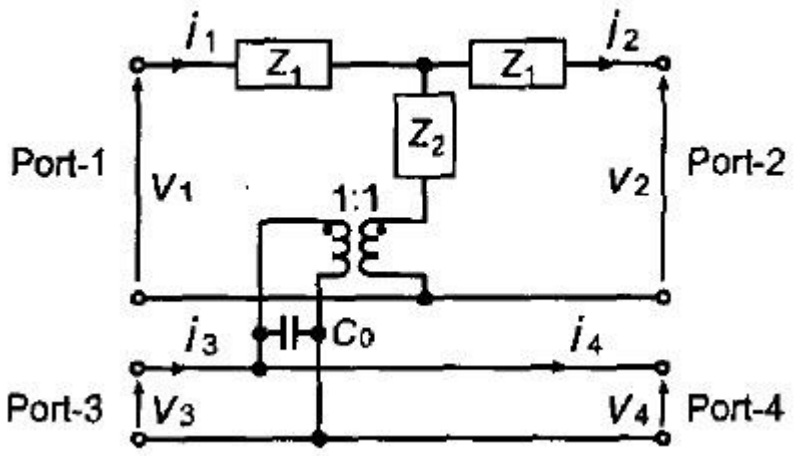

Figure 3.4 Equivalent circuit model for one finger.

Where, G_o is characteristic admittance; R_o= $1/G_o$; F_s, and Υ_s, are image parameters. From the equivalent circuit shown in Fig.3.4, an exchange framework for a

half intermittent area of IDT is inferred through circuit investigation as demonstrated in (3.5).

$$\begin{bmatrix} \upsilon_1 \\ i_1 \\ \upsilon_3 \\ i_3 \end{bmatrix} = \begin{bmatrix} a_{11} & a_{12} & a_{13} & 0 \\ a_{21} & a_{22} & a_{23} & 0 \\ 0 & 0 & 1 & 0 \\ a_{41} & a_{42} & a_{43} & 1 \end{bmatrix} \begin{bmatrix} \upsilon_2 \\ i_2 \\ \upsilon_4 \\ i_4 \end{bmatrix} \tag{3.5}$$

where

$$\begin{cases} a_{11} = a_{22} = cosh(\gamma_s) \\ a_{12} = (R_0 / F_s)\sin h(\gamma_s) \\ a_{13} = a_{42} = \pm(1 - a_{11}) \\ a_{21} = G_0 F_s sinh(\gamma_s) \\ a_{23} = a_{41} = \pm a_{21} \\ a_{43} = j\omega C_0 + G_0 F_s sinh(\gamma_s) \end{cases} \tag{3.6}$$

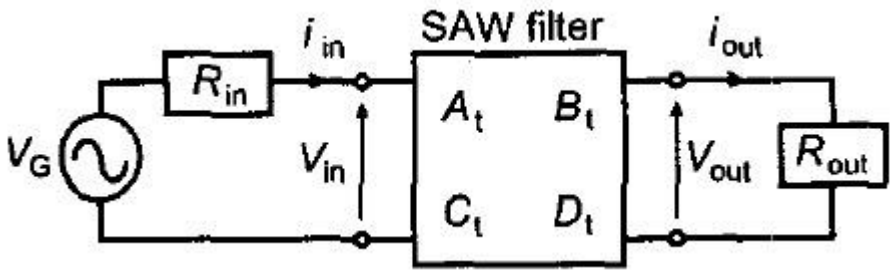

Figure 3.5 Two-port network of the SAW filter.

Bringing the move framework up in (3.5) to the (2N- 1)th power, we acquire an exchange grid for N occasional areas of (IDT-1 and IDT-2). A short time later, on the grounds that these segments are joined acoustically in course, an exchange framework for the entire SAW sensor is additionally acquired as the result of their exchange lattices. [9] Considering terminal conditions for acoustic and electric ports, we can have a scientific model of the three-IDT sort SAW sensor as a two-port system in Fig.3.4

CHAPTER 4

SIMULATION RESULTS

To achieve optimal performance, parameters of device such as substrate thickness, IDT thickness, IDT length, fluid and solid environment tests were done by using ANSYS (ANSYS, Inc, Canonsburg, PA) and COMSOL multiphysics. A two-dimensional and three-dimensional, simulation also was done to check directionality on both solid and liquid surroundings. There are advantages and disadvantages of each simulation software's. First we will follow the instructions of Jeffrey.J.Mcllean [7], and use ANSYS multiphysics with given codes on their appendix side of their work to check directionality concept. Secondly we will change some parameters and arrangements and that's why we will be using COMSOL multiphysics.

4.1 DEVELOMPENT OF FINITE ELEMENT MODEL

To understand how to model our device settings in ANSYS simulation software we have to confirm wave generation in both fluid and solid. For this test we can use baffled piston radiation. This closed structure arrangement can be very good concept to understand fluid structure interaction problem. So in this problem silicon substrate is placed inside of liquid to generate waves on the surface of elastic medium by a result of solid fluid interaction. By examining this problem and improving some parts of arrangement we can get idea of how one single metal thin IDT can be modeled . [7]

4.2 ANALYSIS OF BAFFLED PISTON

As we stated above, to check if the acoustic wave generated on top of elastic medium inside with fluid structure interaction, baffled piston problem was tested first. This model contains four main parts: the solid medium, liquid medium, fluis solid interaction also known as FSI and absorbing boundary. The model of baffled piston problem is delineated in the figure 4.1. The trickiest part is absorbing boundary part, as it illustrates the liquid which is going to infinity. For our luck we have this kind of ready absorbing boundary arrangement in ANSYS. [7]

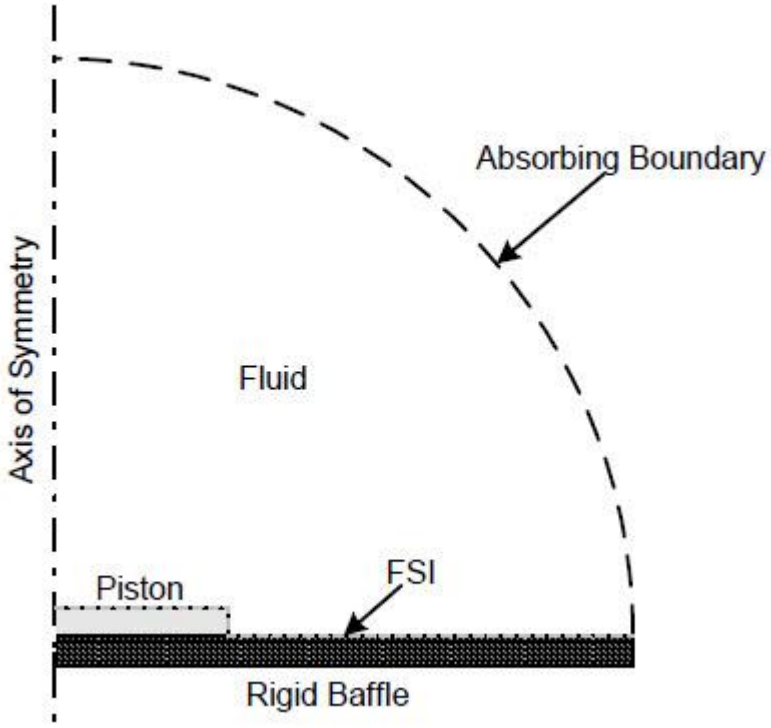

Figure 4.1 Illustration of the model of a vibrating piston on a baffle.

For the fluid part, Fluid 29 component of software was used. This fluid has all properties that is needed. When solid is vibrated, the vibration is summoned with the liquid. Two way coupling from the liquid to the solid and the reverse will be the result of this vibration. [7]

As we stated before the absorbing boundary part is the trickiest part. Assumption is that the liquid goes to infinity in order not to cause any standing wave ration or reflecting waves which can affect simulation results very badly. It is not a secret that we always take in assumption to that our components be like perfect in theory or simulations not like in real practice. That's why here we use absorbing boundary condition.

This permits one to reenact a vast liquid space with a limited number of elements. The absorbing boundary condition obliges that the limit of the liquid area be a fragment of a circular arc.

Baffle is rigid, inflexible medium. The substance of the cylinder is compelled to have a y displacement at the consonant excitation recurrence. The model was then fathomed more than a scope of frequencies.

Figure 4.2 is the plot of radiation impedance of analytical and FEM results for baffled piston vibration model. Where bold line speaks to the FEM results and analytical ones shown with the dashed line [7]

From result we can see that FEM result is good up to 2ka and after this the outcomes starts to hint a deficient. This deficient actually speaks to the mesh deficient:

$$\lambda_{fluid} = \frac{C_{fluid}}{f} \tag{4.1}$$

Where λ_{fluid} is the wavelength of the acoustic wave in the liquid, c_{fluid} is the speed of sound, furthermore, f is the frequency of excitation. For a cylinder with a radius of 15μm, an estimation of 2ka of 5 relates to a frequency of almost 40 MHz. For this [7]

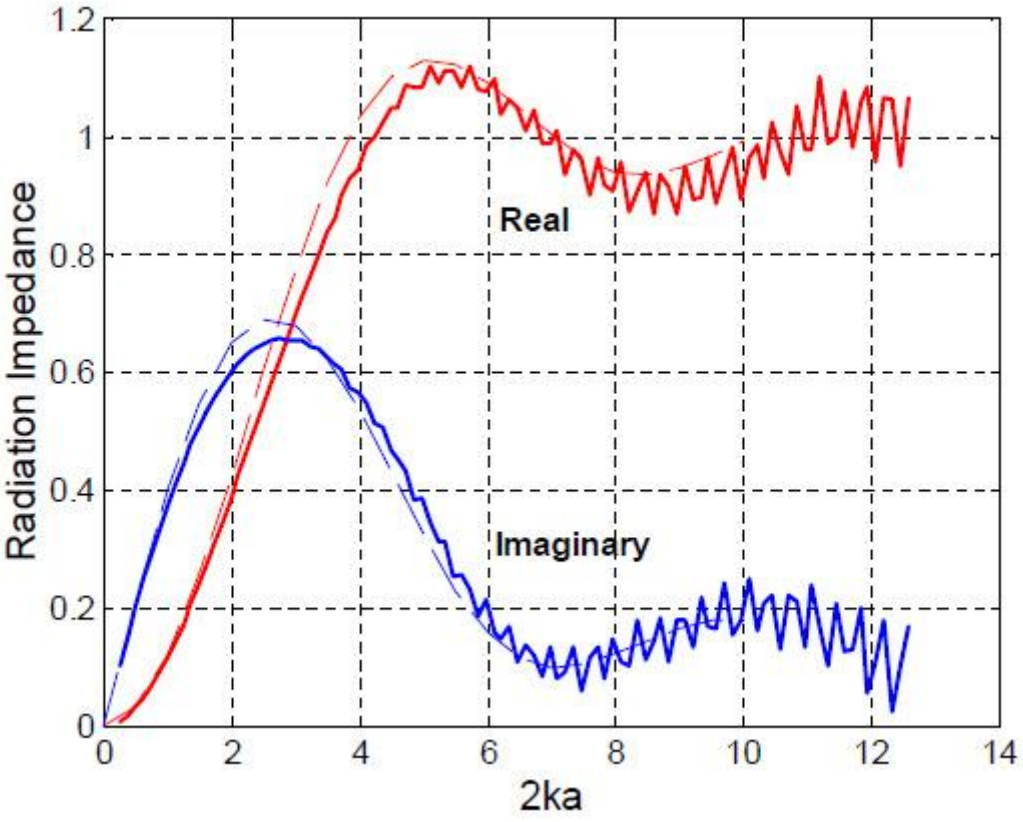

Figure 4.2 Radiation Impedance of analytical and FEM result.

From Figure 4.2, one can see that this speaks to the minimum mesh density needed to get precise results in the acoustic examination. After this basic esteem, the model starts to separate because of inadequate mesh density

The results say that our assumption of baffled piston model worked properly. The absorbing boundary condition and FSI or fluid structure interaction of ANSYS also gave some good results. The outcomes likewise settled that the minimum mesh density for the liquid to create good acoustic model must be no less than 15 components per wavelength. Next, step is to apply these results to model unidirectional SAW metal thin electrode IDT's to generate surface acoustic wave on top of elastic substrate. [7]

.

4.3 SIMULATION OF ITERDIGITAL cMUT ARRAY IN FLUID HALF-SPACE

Subsequent to checking the operation of the fundamental finite element model, an interdigital cMUT (capacitively micromachining ultrasonic transducer) array was brought into the model of a liquid half-space connected to a silicon plate, as demonstrated in Figure 4.3

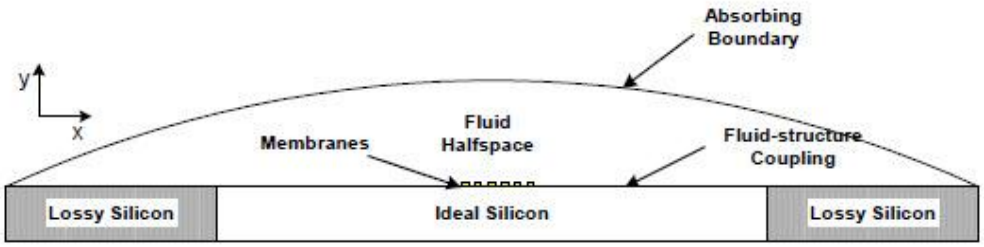

Figure 4.3 Illustration of finite element model for fluid half-space.

The membranes were energized by force connected to the nodes with the goal that complex loads could be connected to simulate the wanted 90º phase shift. All simulations were performed at a frequency of 10MHz.

A 5 finger pair, interdigital cMUT was simulated in a liquid half-space. The subsequent pressure circulations in the liquid for the transducer working at 10MHz on a 200μm silicon substrate are demonstrated in Figure 4.4

The outcomes demonstrate the capacity to produce exceedingly directional Scholte waves in the liquid, which show up as fleeting waves in the vertical direction while propagation in the horizontal direction as planar wave fronts. By changing the phase of the inputs, one can produce a profoundly directional Scholte wave in either lateral direction [7].

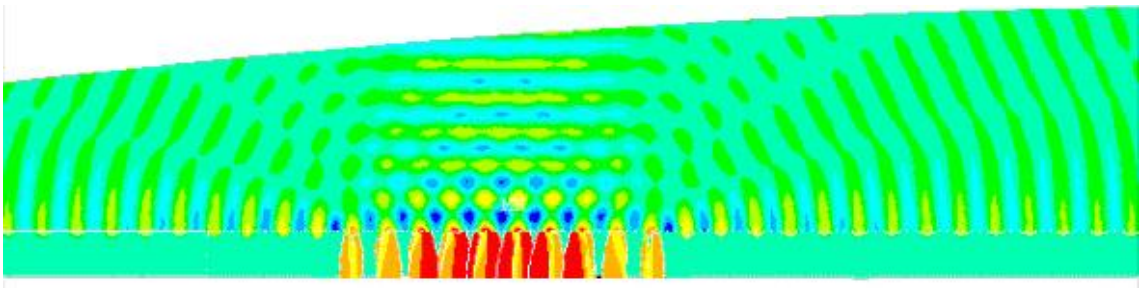

(a)

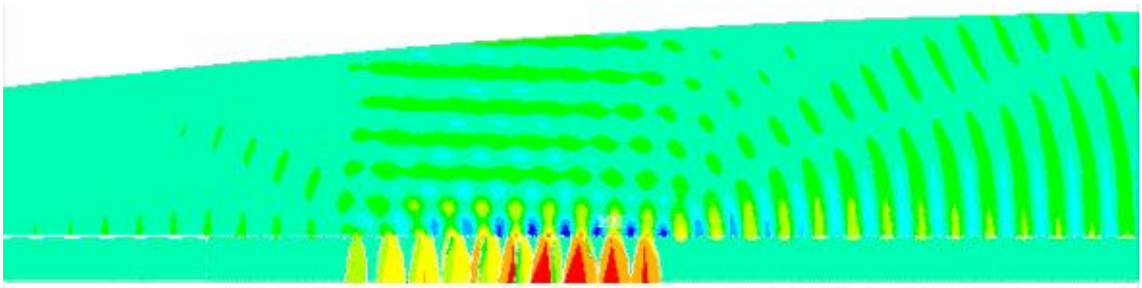

(b)

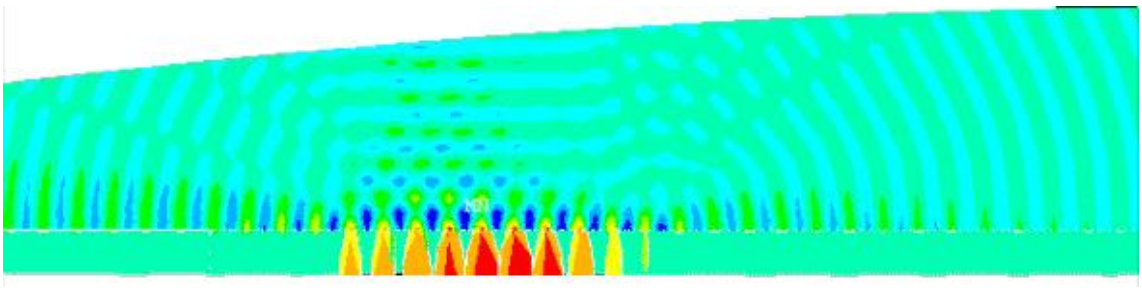

(c)

Figure 4.4 Fem results for : (a) in phase, (b) -90° out of phase, and (c) +90° out of phase.

4.4 SIMULATION VIA COMSOL MULTIPHYSICS

Previous simulations were just a kind of emulation of real simulation that is going to be done. The purpose was to proof mathematical or analytical concept. Since, we could proof that and observe that the unidirectionality works, next step is to change material like; silicon to piezoelectric material, membrane to aluminum electrode and instead of liquid air will be provided. After, several parametric studies was performed to observe directionality of surface acoustic waves on a piezoelectric substrate.

4.4.1 Parametric Study

Several parametric studies have been done. As seen in figure 4.5 there is lot of parameters which should be considered during designing 3-port SAW sensor, like; number of IDT's, height of IDT's, length of IDT's (in 3D simulation there is extra parameter called length of overlap of IDT's), distance between neighboring IDT's, distance from horizontal wall of substrate, delay or distance between transmitter array and receiver arrays, thickness and width of piezoelectric substrate.

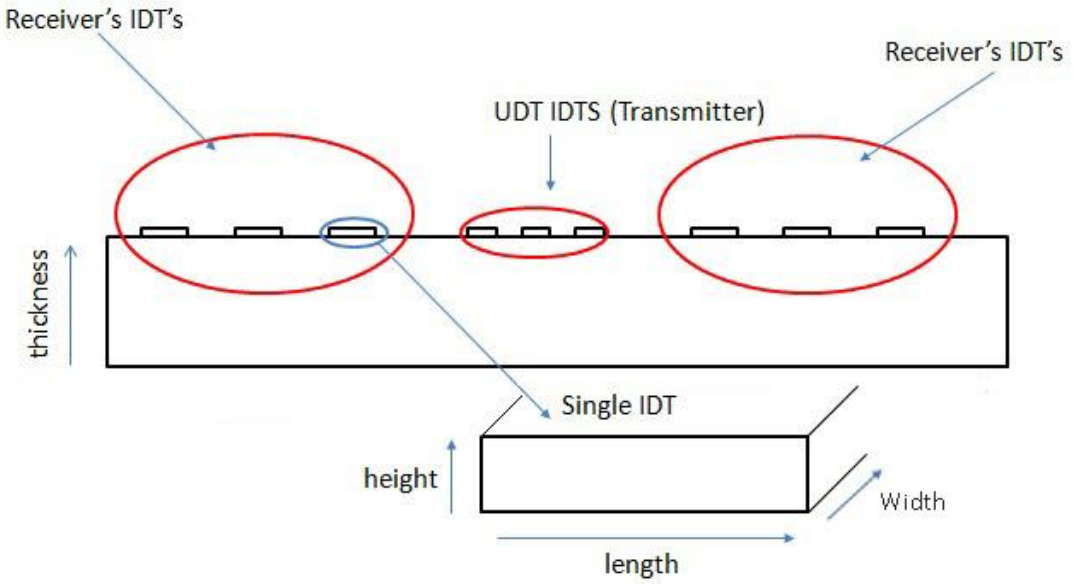

Figure 4.5 3-port SAW sensor.

First, let us check the directionality of our design, if it is working bi-directional or unidirectional when electric potential is applied to the transmitter array of IDT's. So we apply Acos(wt) to one leg of transmitter array and Asin(wt) to another leg of transmitter array and vice-versa.

When electric potential is applied to transmitter array, output signal is derived from probes connected to left (states for backward propagation of SAW) and right (forward propagation of SAW) receiver IDT's. And from figure 4.6 we can see that our design is working properly

Next step is the length of receiver (bidirectional) IDT's from λ/8 to λ/4. As seen in figure 4.7, when we change thickness of reciever IDT's there is no a big difference in output signal, but λ/4 is little bit better.

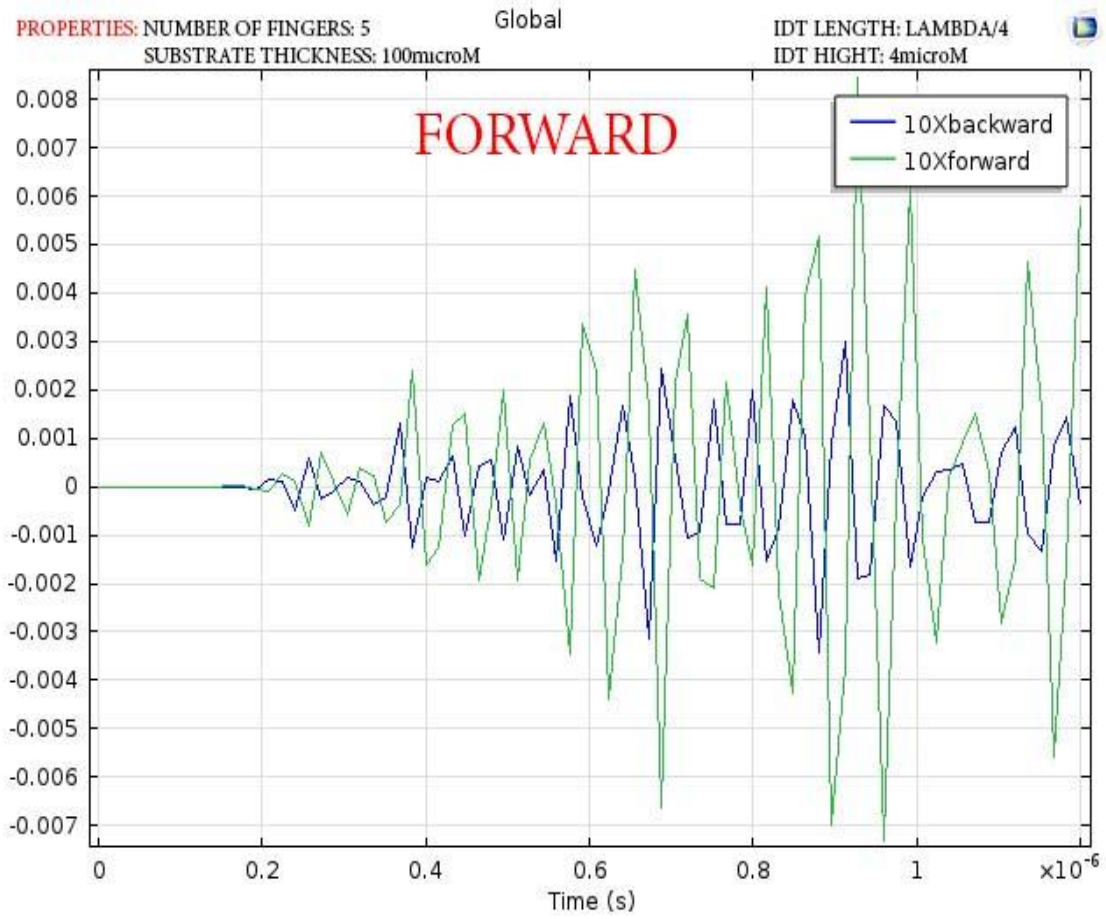

(a) Forward

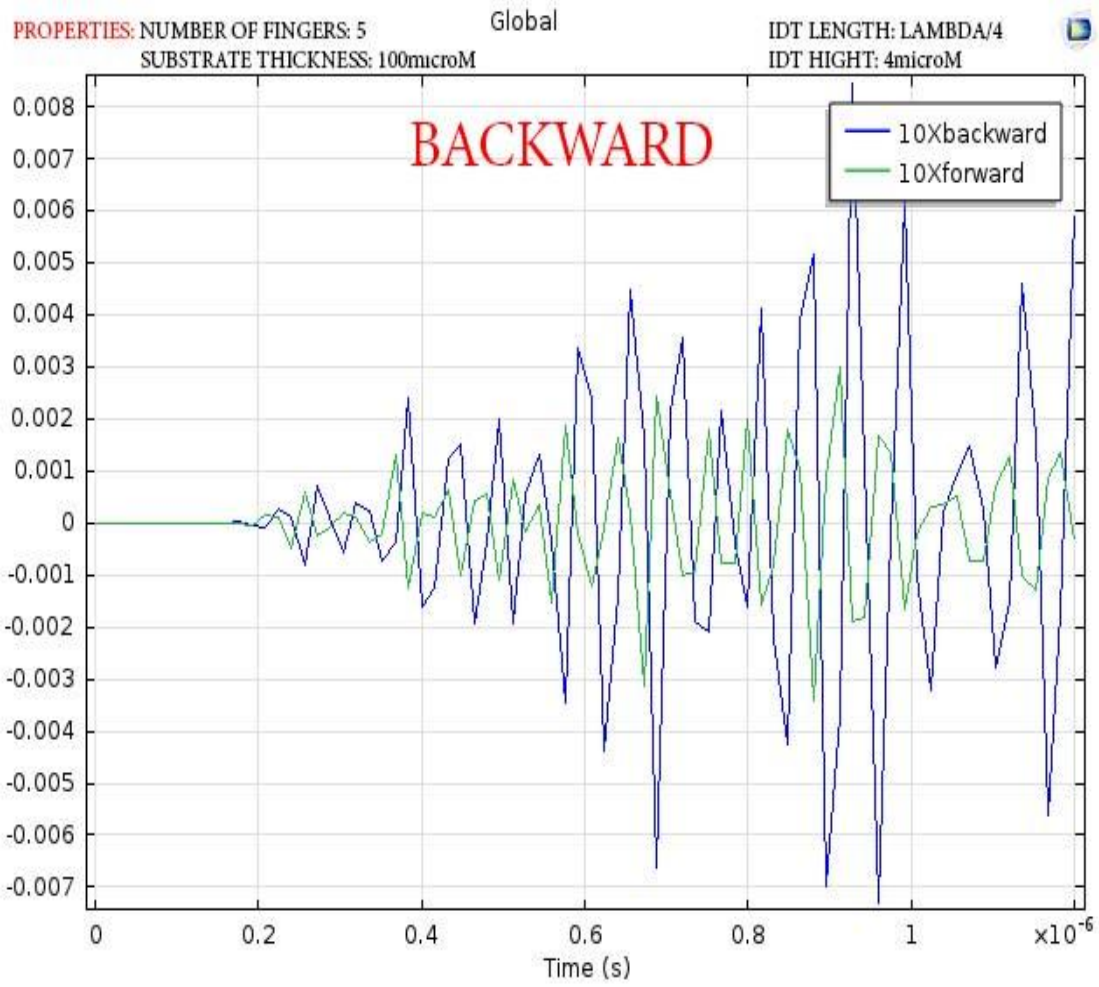

(b) Backward

Figure 4.6 (a) forward propagation of SAW (b) backward propagation of SAW.

Next, we will change number of finger pairs from 5 to 10 (for transmitter array) and see the result in figure 4.8. From figure 4.8 we can do deduction that there is no difference between 5 finger pair transmitter array and 10 finger pair transmitter array. But, as we state in previous chapters the selectivity shoudl increase as number of fingers rise. We can do a simple deduction, first we replaced liquid with air and another reason can be 2-D simulation

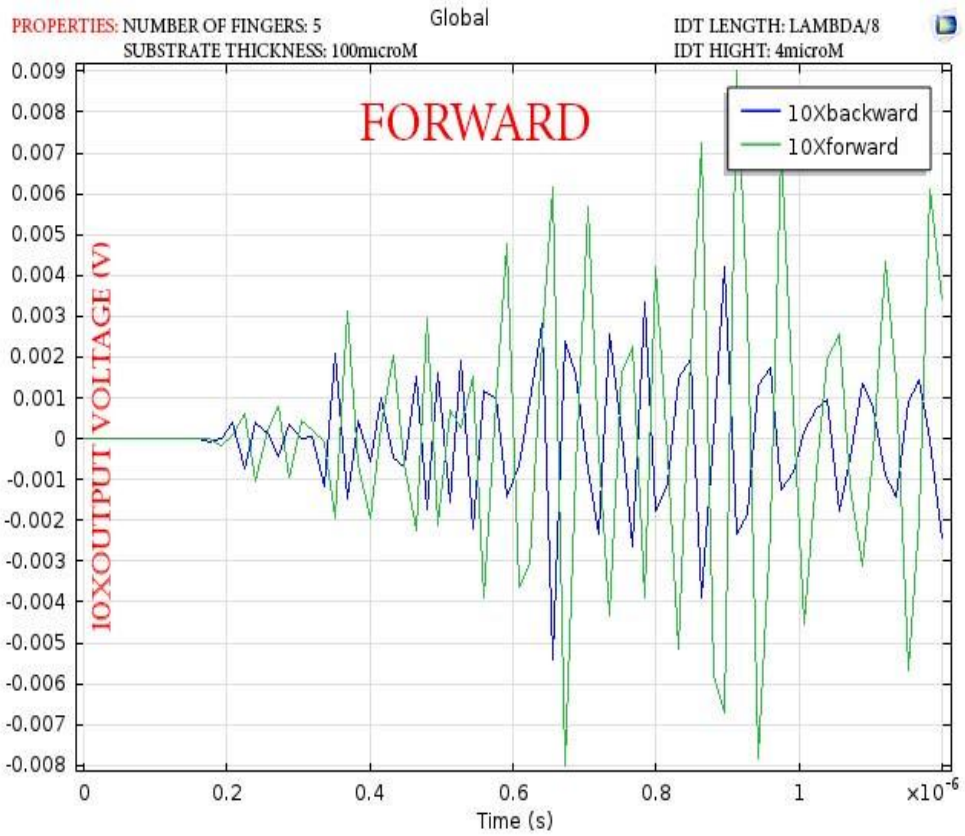

(a)

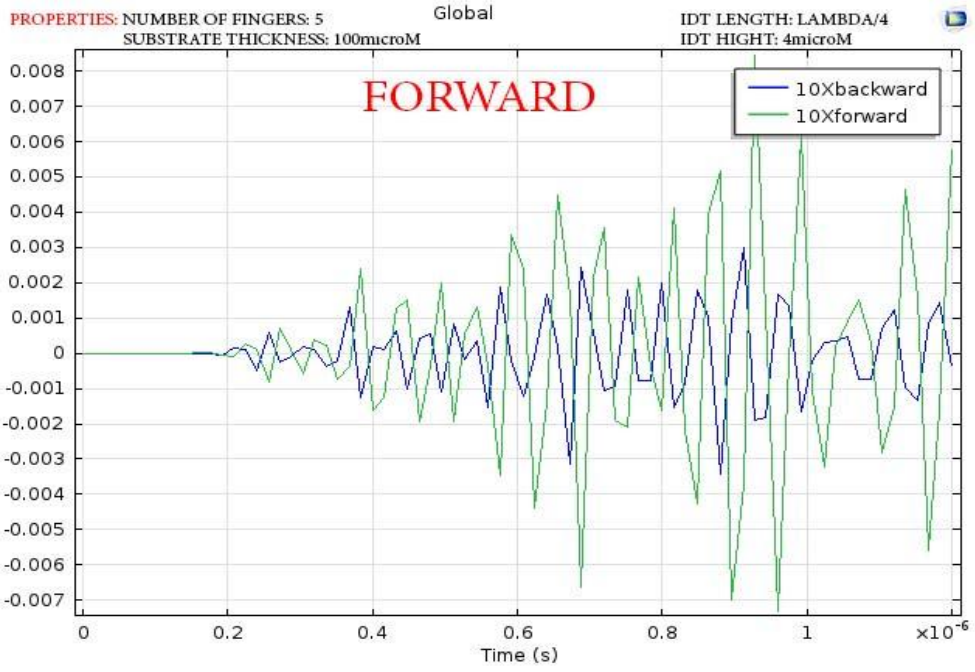

(b)

Figure 4.7 Length of reciever IDT's (a) λ/8 (b) λ/4.

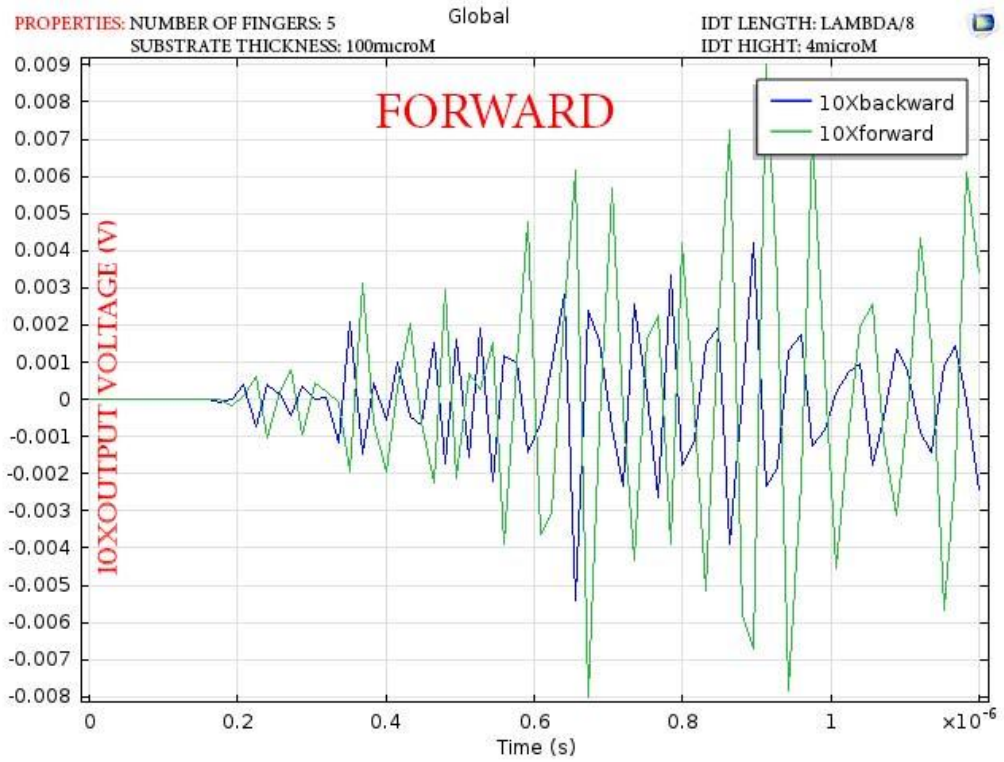

(a)

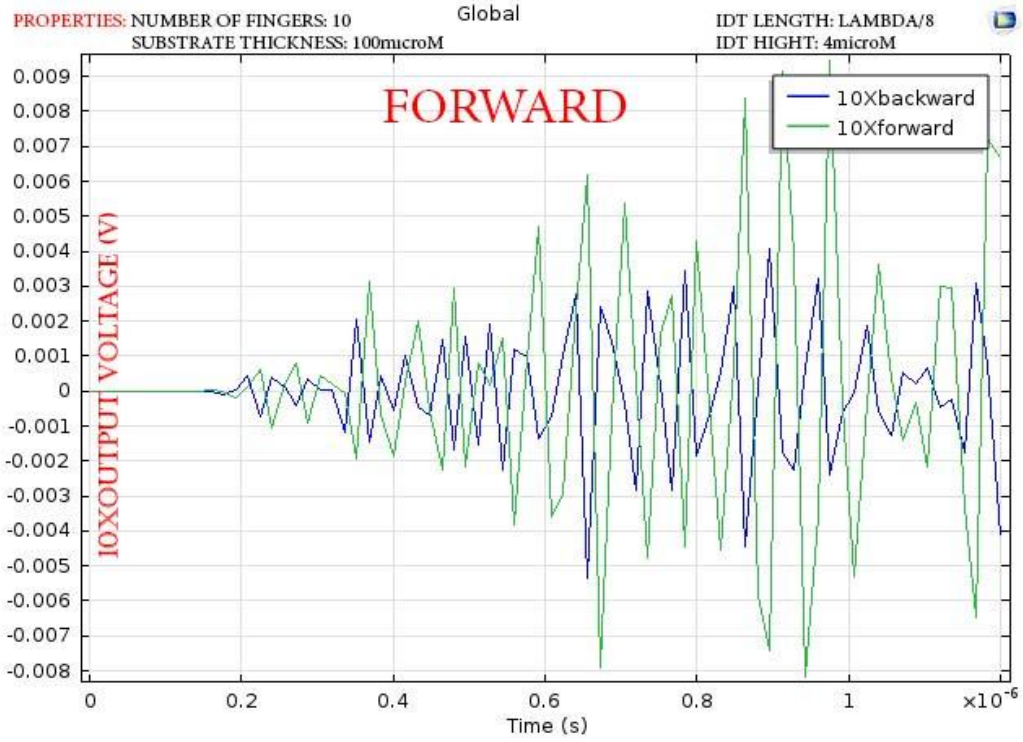

(b)

Figure 4.8 Number of finger pairs (a) 5 finger pairs (b) 10 finger pairs.

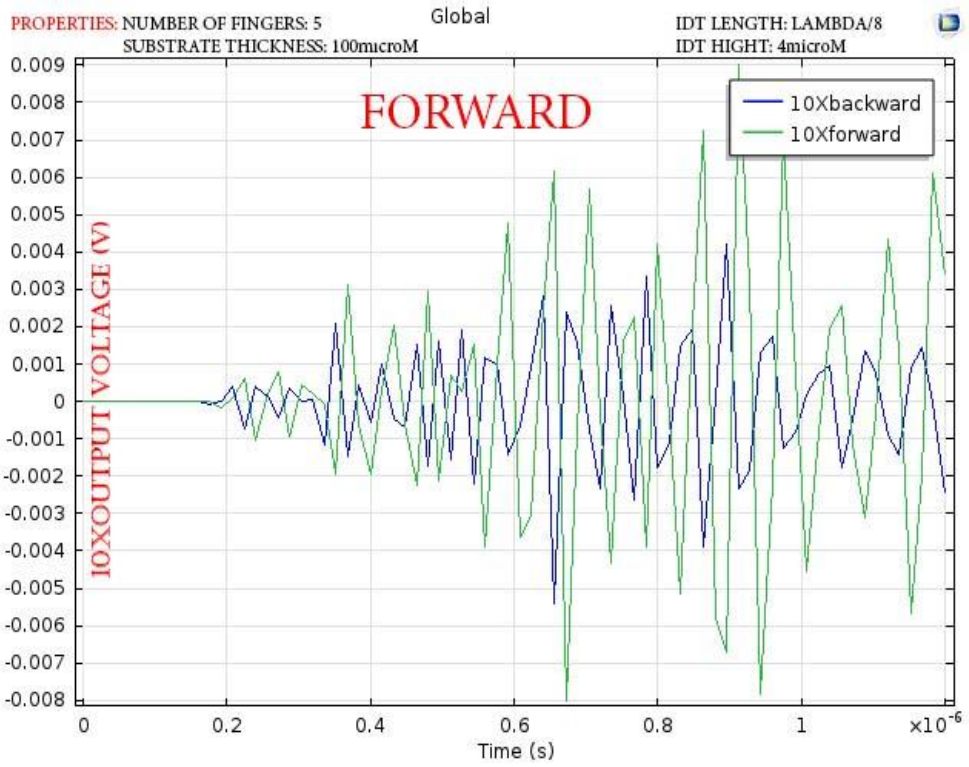

(a)

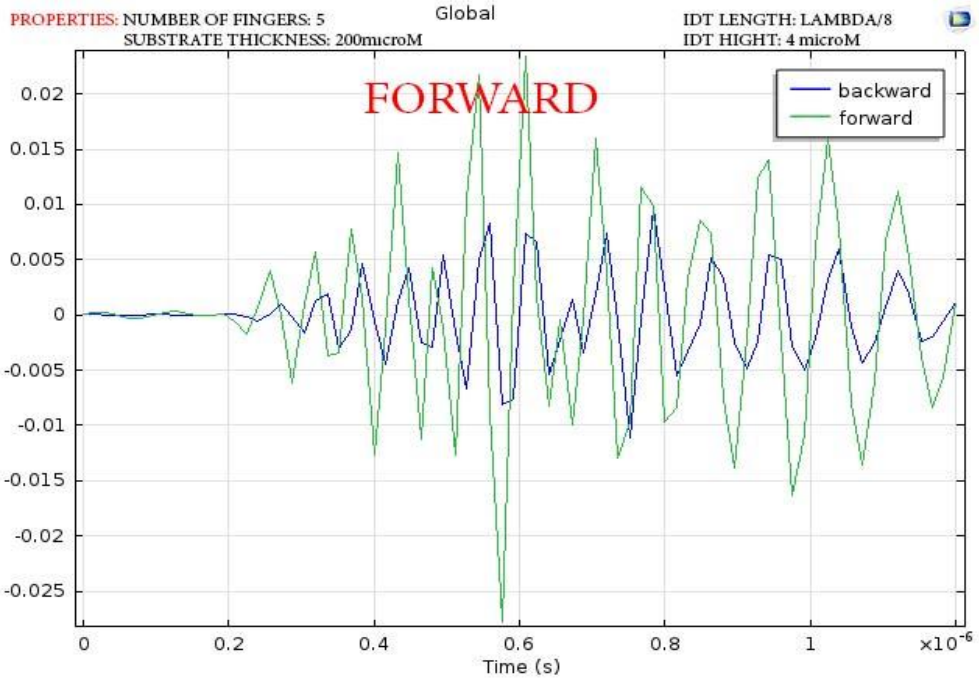

(b)

Figure 4.9 Substrate thickness (a) 100 micrometer (b) 200 micrometer.

From figure 4.9 we can see that 200 micrometer piezoelectric substrate is much more better than 100 micrometer one.

Effect of IDT's height in generation of unidirectional surface acoustic waves going to be observed. From figure 4.10 we can see, effect is linearly proportional to the height of IDT. Which means, as height increases the power of signal also increases. But we know that after some values, in practice IDT's are going to acts as rigid structure. Also, in our lab we can go up to 200 nm, that's why while designing we have chosen that value.

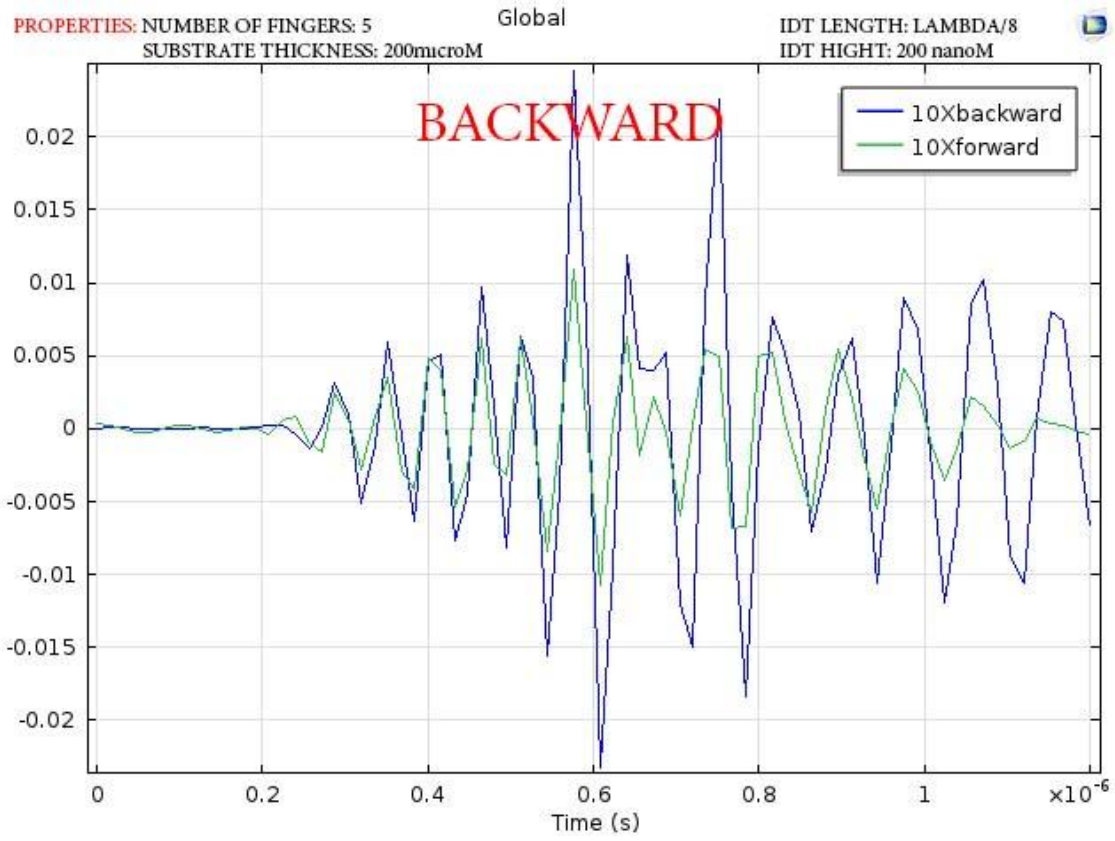

(a)

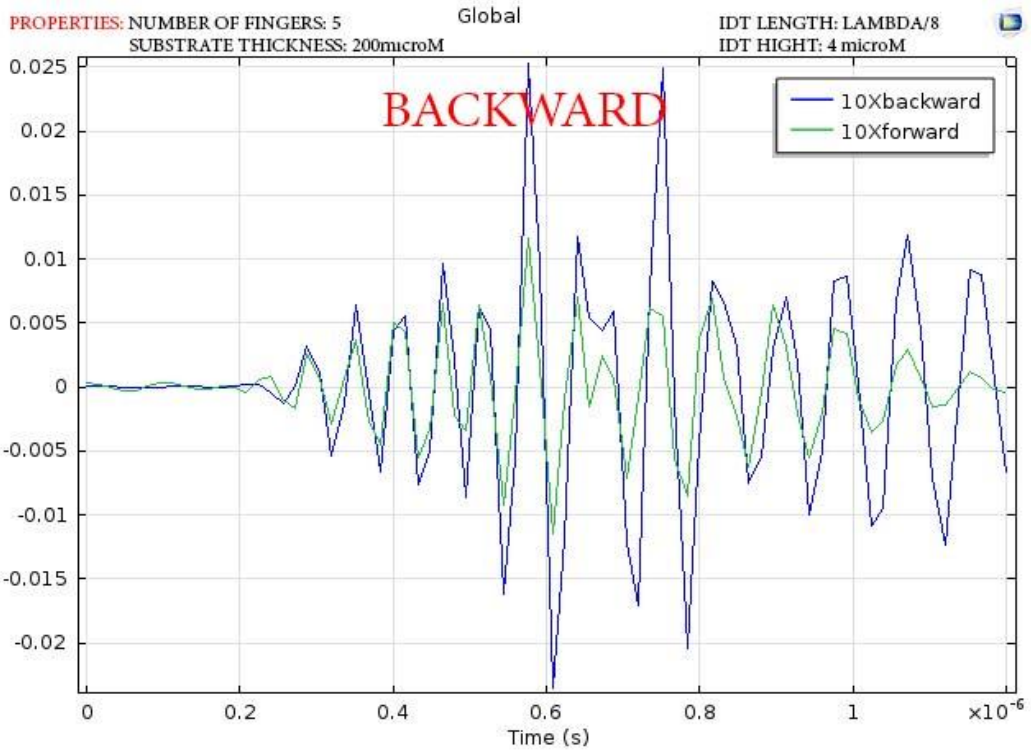

(b)

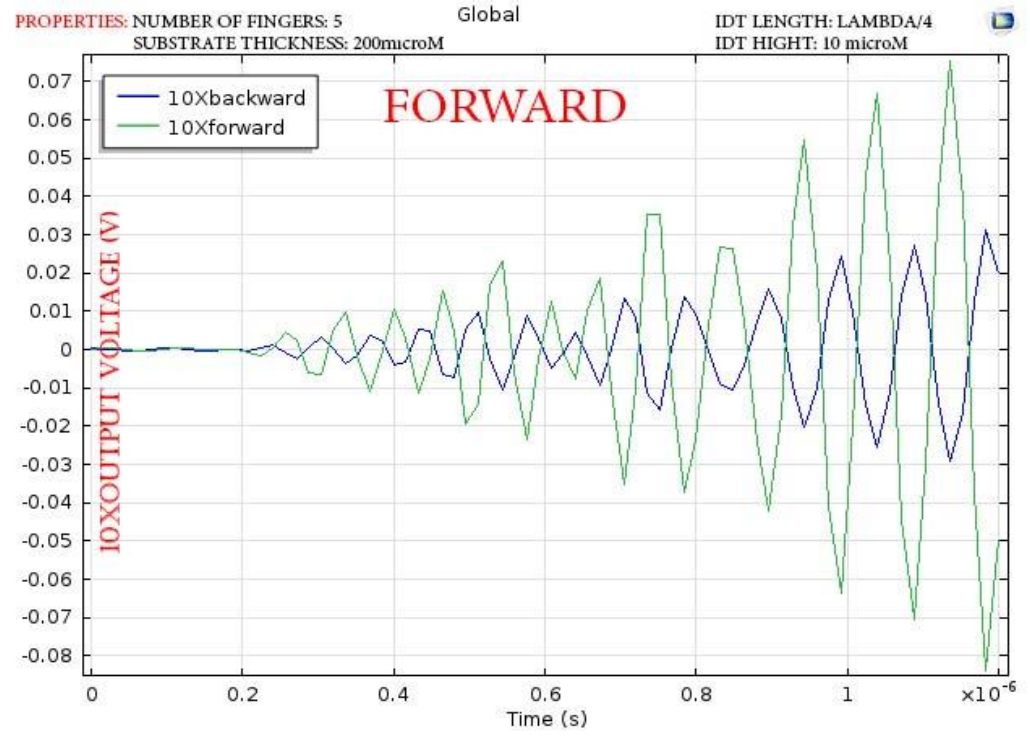

(c)

Figure 4.10 (a) IDT height 200 nm (b) 4 micrometer (c) 10 micrometer.

During experiments we observed some kind of reflection point, which is caused by distance between piezoelectric substrate wall and receiver IDT array and delay (distance between transmitter and receiver arrays).

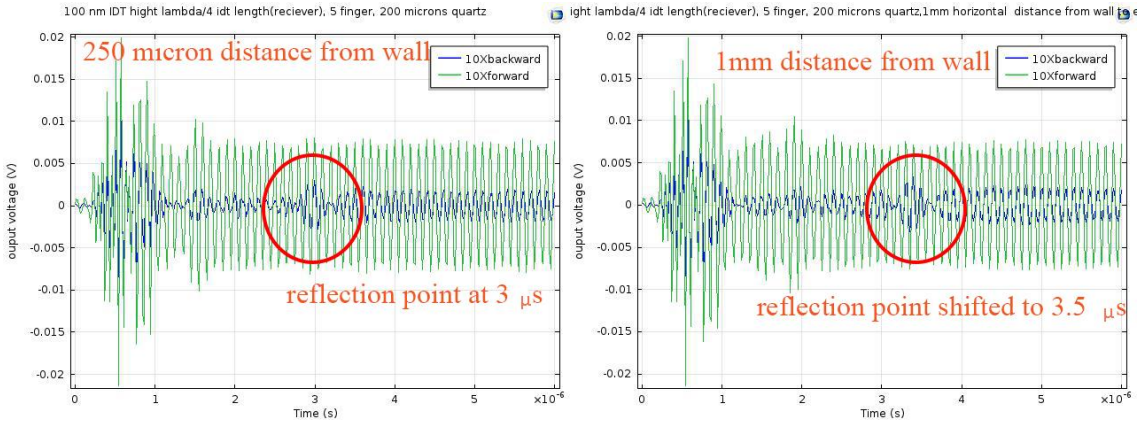

Figure 4.11 distance from wall is 1mm.

In figure above, the shift in reflection point can be observed as distance from wall increases. Since we increased further up to 3mm as seen in figure 4.13

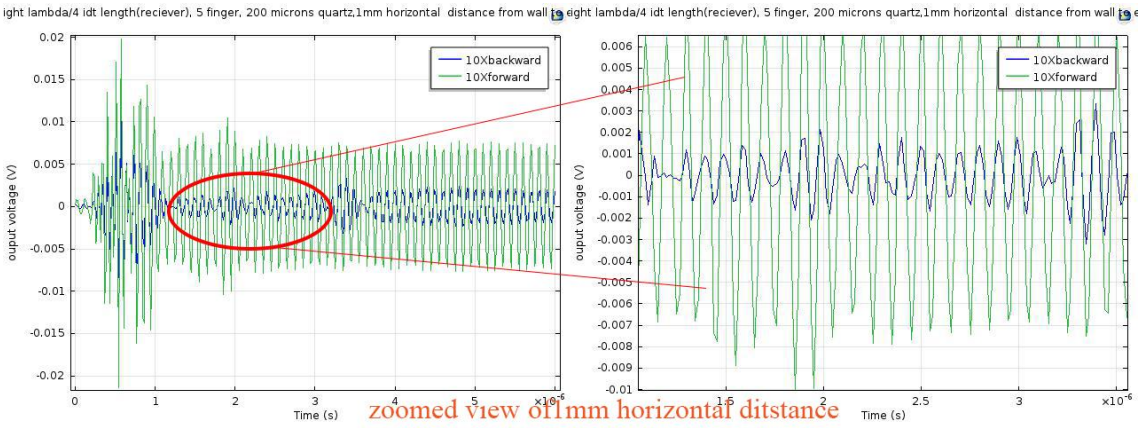

Figure 4.12 zoomed view of signal (1mm distance from wall).

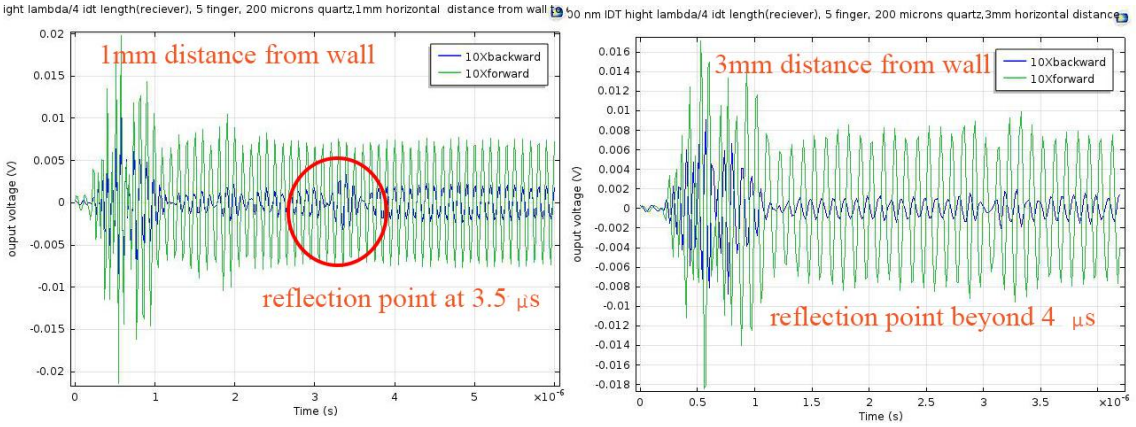

Figure 4.13 distance from wall is 3mm.

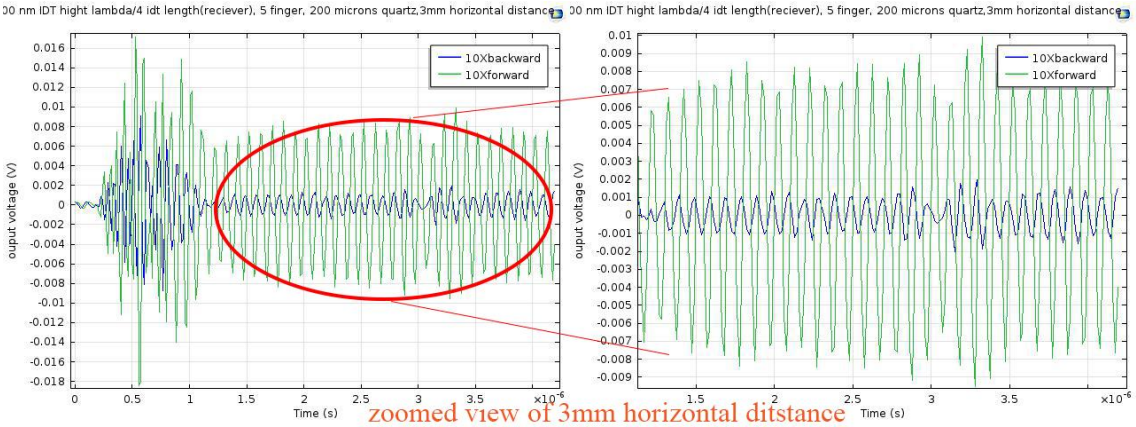

Figure 4.14 zoomed view of signal (3mm distance from wall).

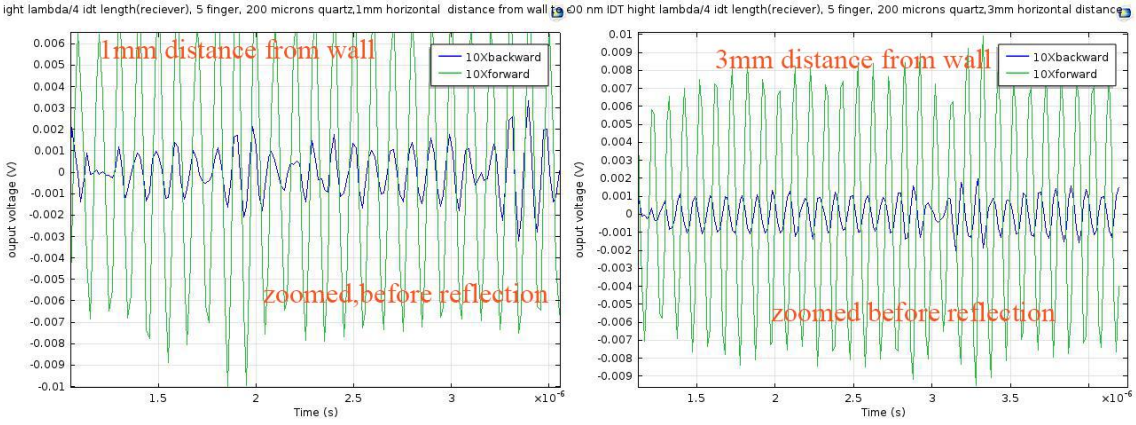

Figure 4.15 comparing 1mm and 3 mm distance from wall.

Up to this point we were increasing distance of receiver IDT array from wall of piezoelectric substrate. Next thing we are going to do is increase delay or in other words distance between TX (transmitter array) and RX (receiver array). As seen in following figure 4.16, the reflection point again increases as we increases delay.

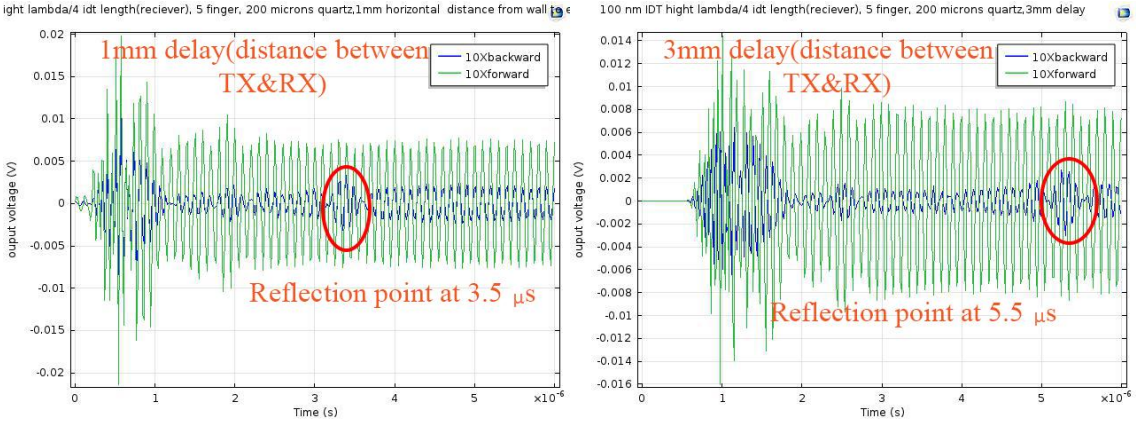

(a)

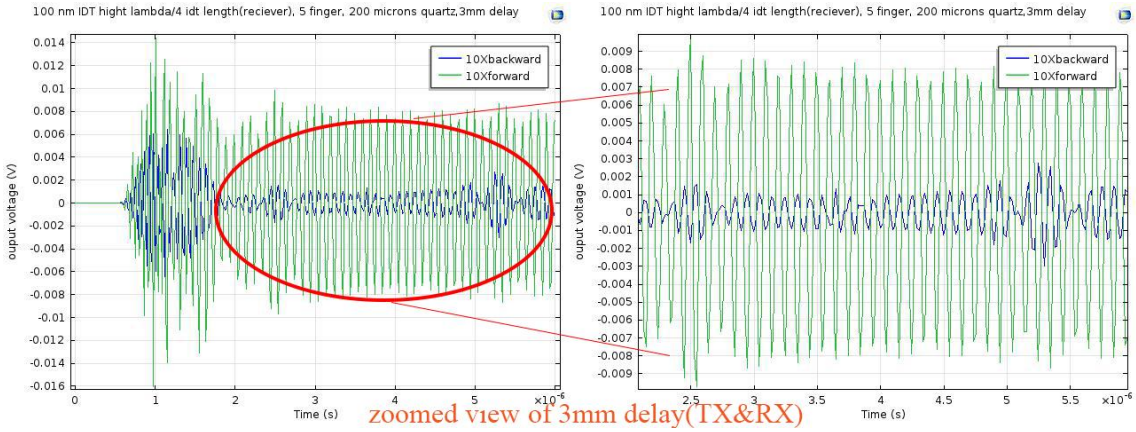

(b)

Figure 4.16 Delay between TX and RX (a) delay is 3 mm (b) zoomed view of 3 mm delay.

We also observed that directionality of surface acoustic waves changes with respect to the thickness of substrate. We assume that optimal substrate thickness value is $\lambda/2$ where it reaches its resonant frequency and surface acoustic waves most efficient. Where λ is target wavelength.

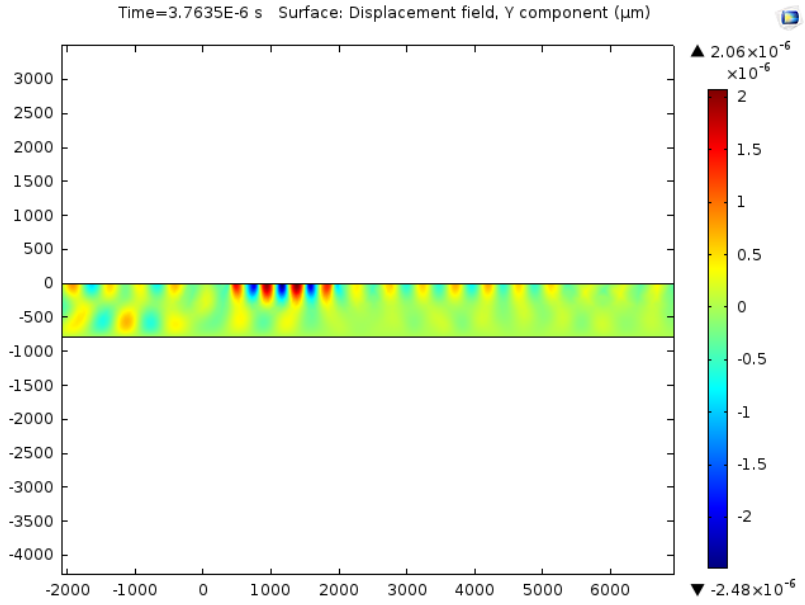

(a)

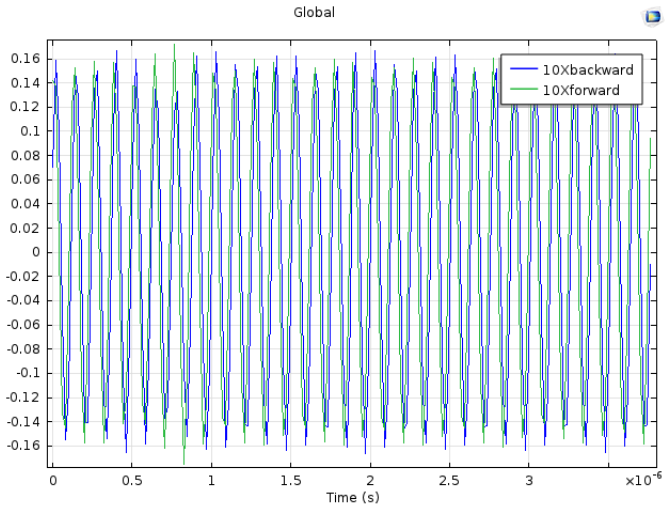

(b)

Figure 4.17 Substrate thickness is 800 microns which is equal to 2λ a) 2D simulatiıon result b) signaloutput.

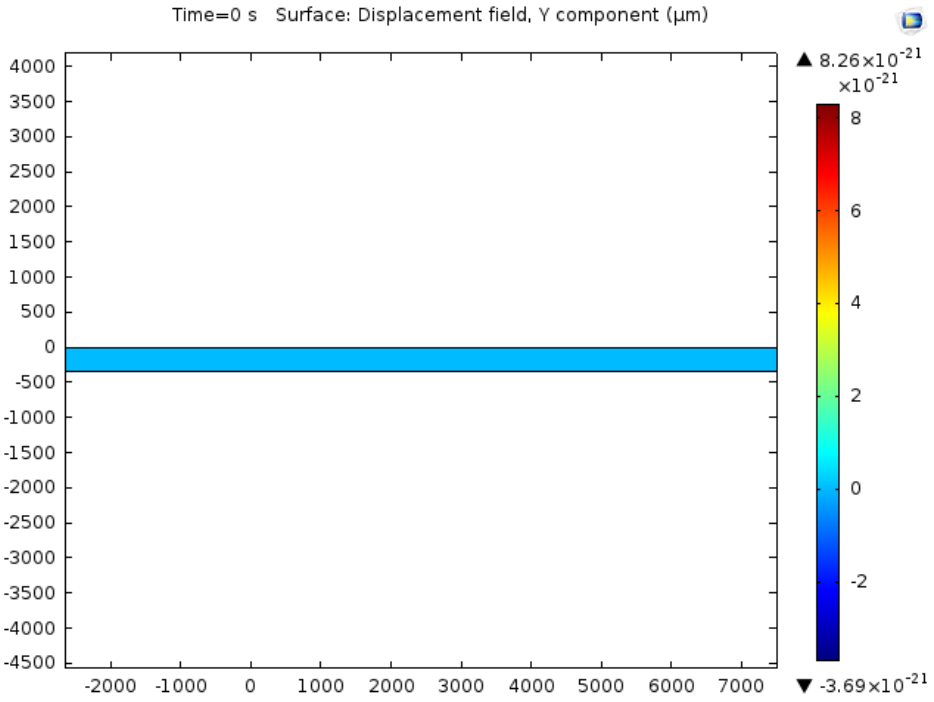

(a)

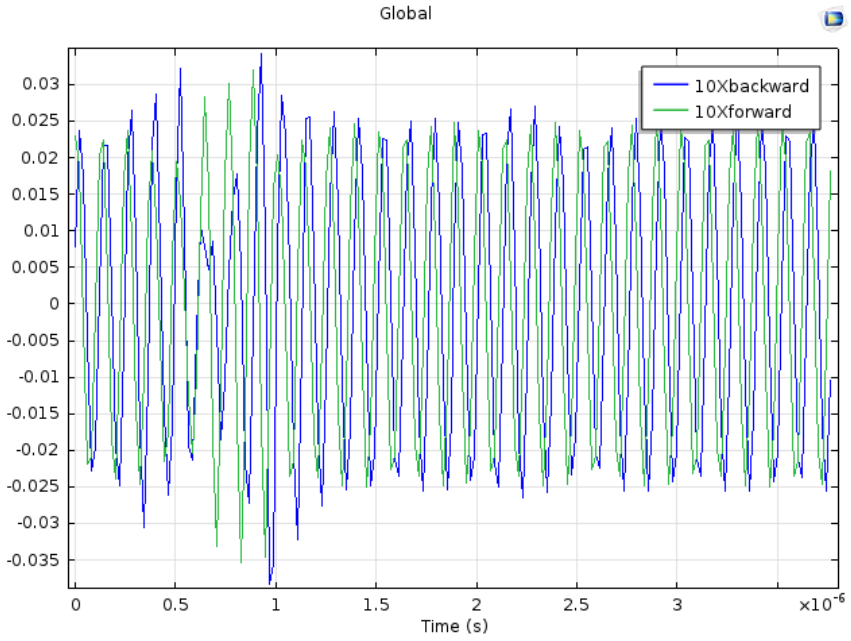

(b)

Figure 4.18 Substrate thickness is 400 microns a) 2D simulatiıon result b) signaloutput.

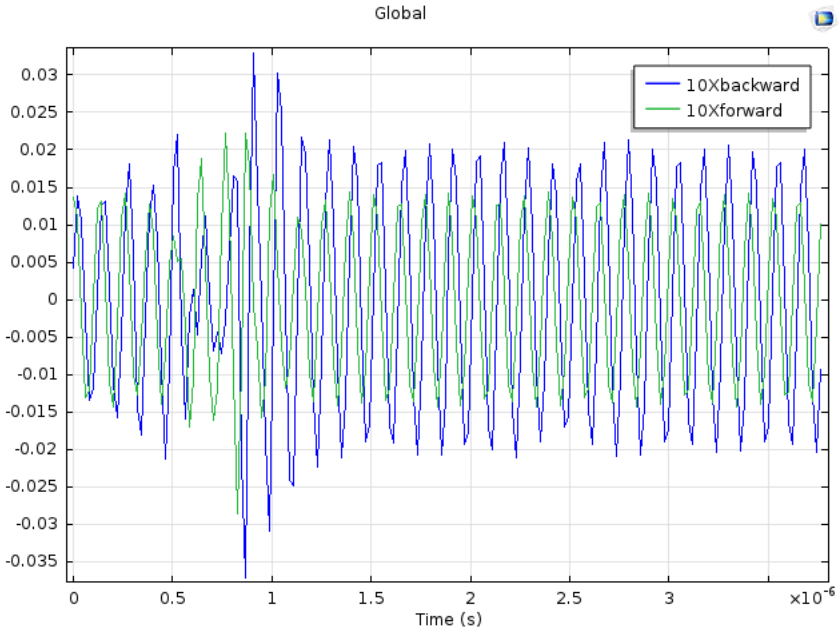

Figure 4.19 Substrate thickness is 350 microns signaloutput.

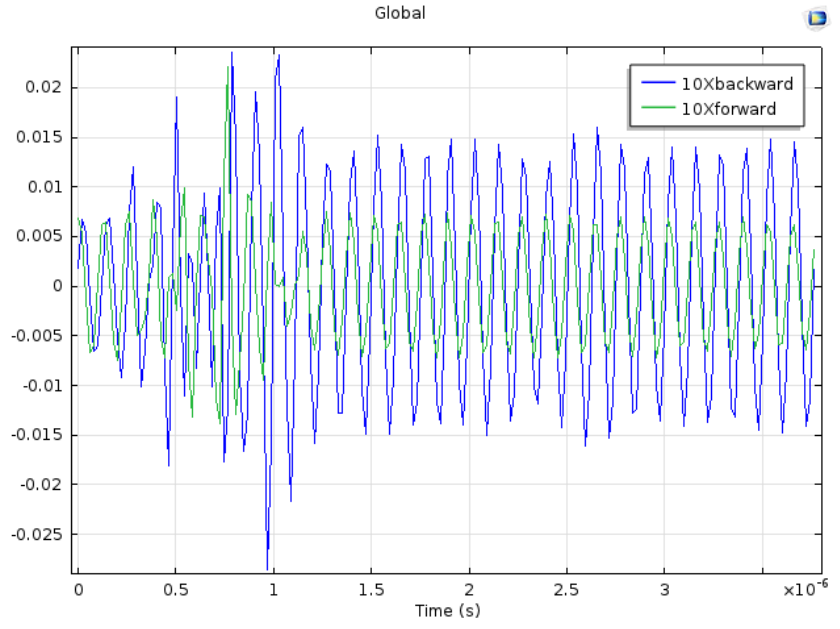

7 Figure 4.20 Substrate thickness is 300 microns signaloutput.

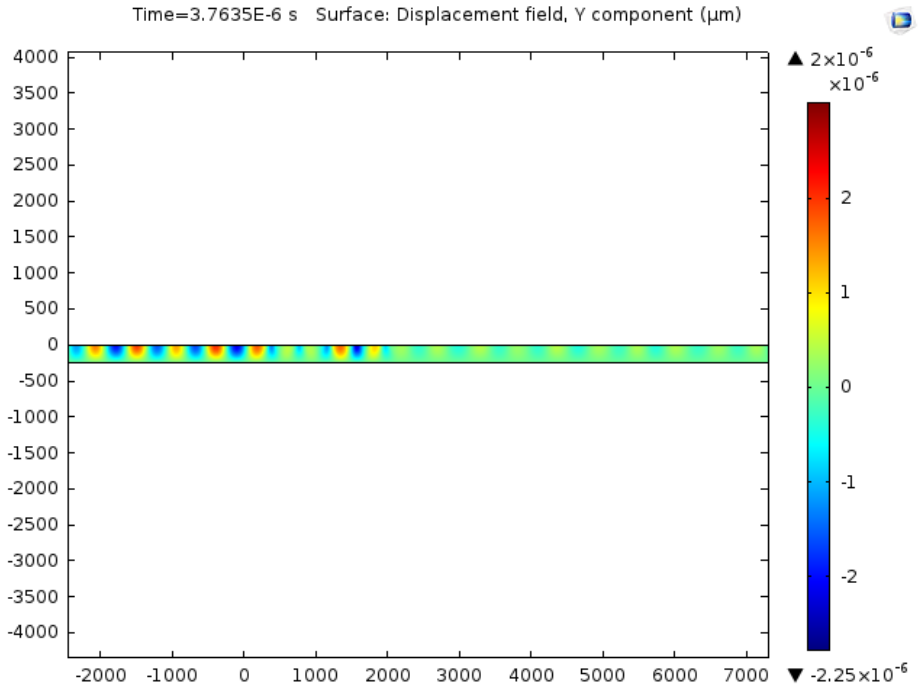

(a)

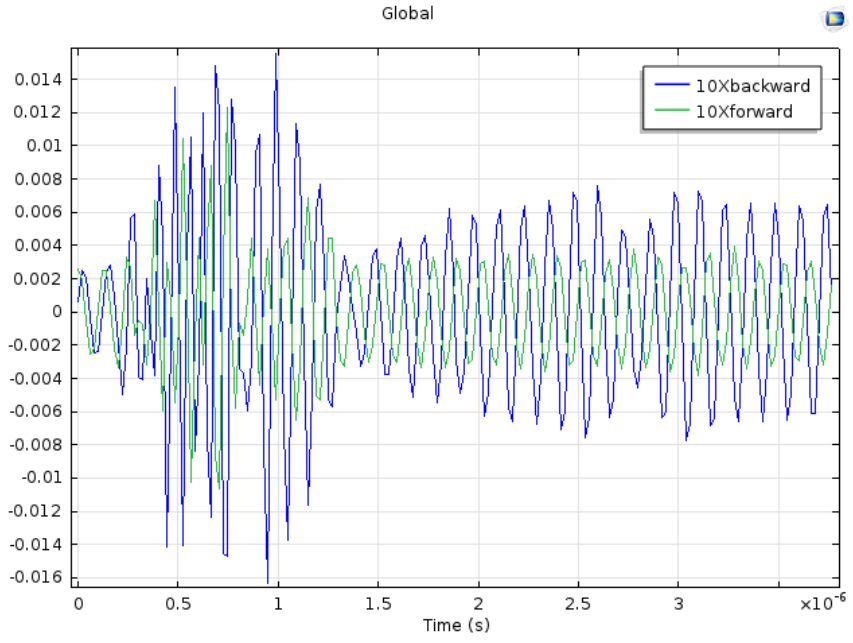

(b)

Figure 4.21 Substrate thickness is 250 microns a) 2D simulatiıon result b) signaloutput.

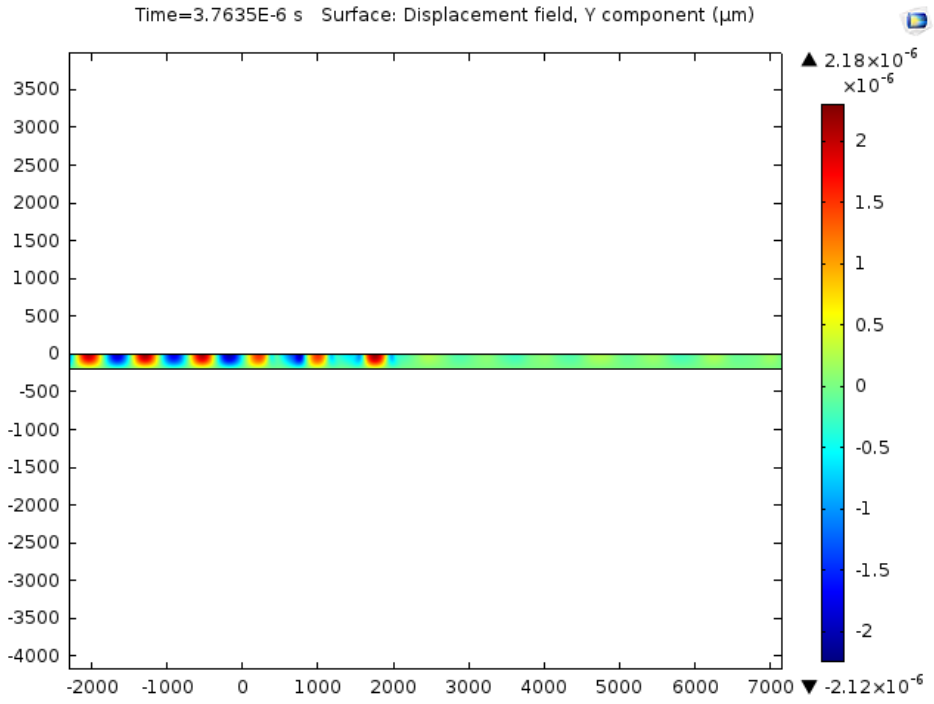

(a)

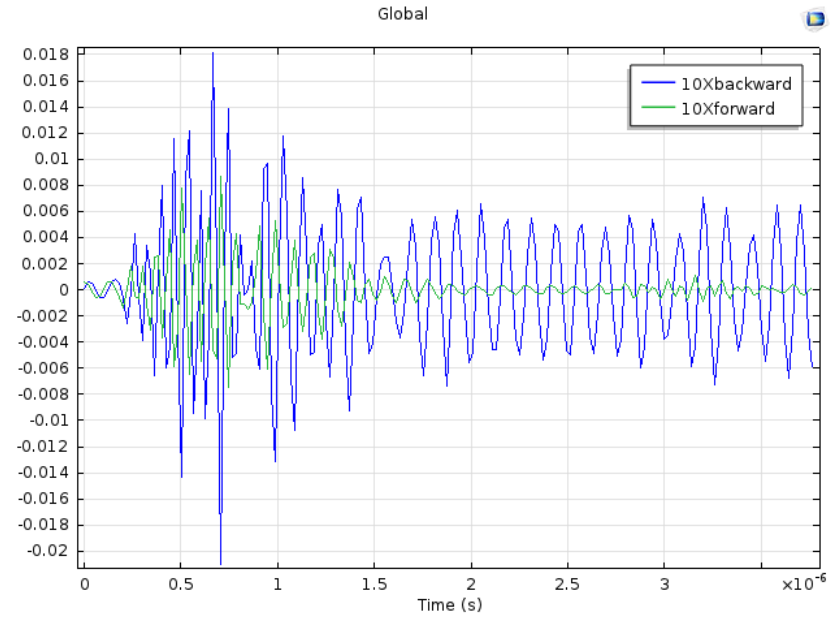

(b)

Figure 4.22 Substrate thickness is 200 microns whic is equal to λ/2 a) 2D simulatiıon result b) signaloutput.

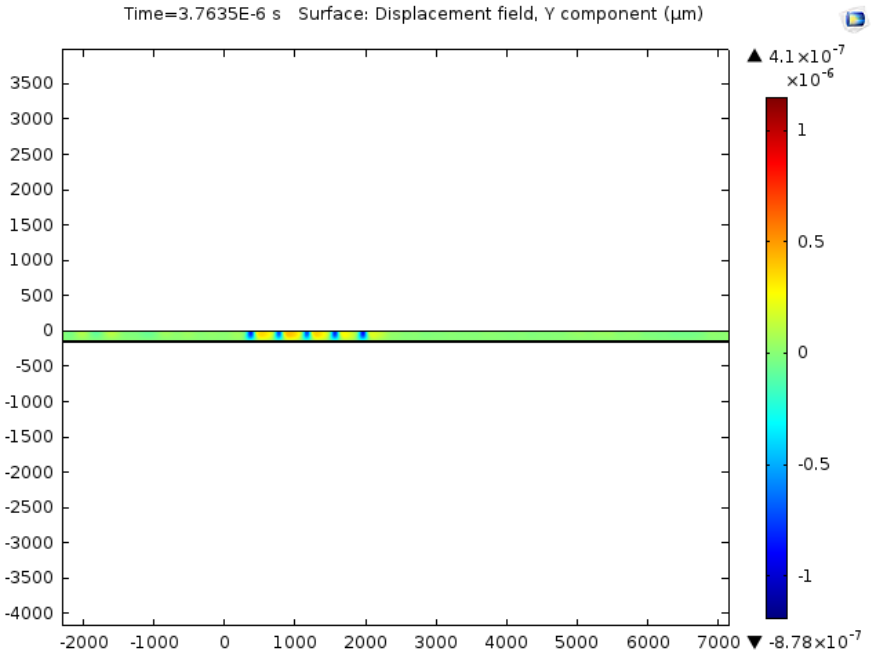

(a)

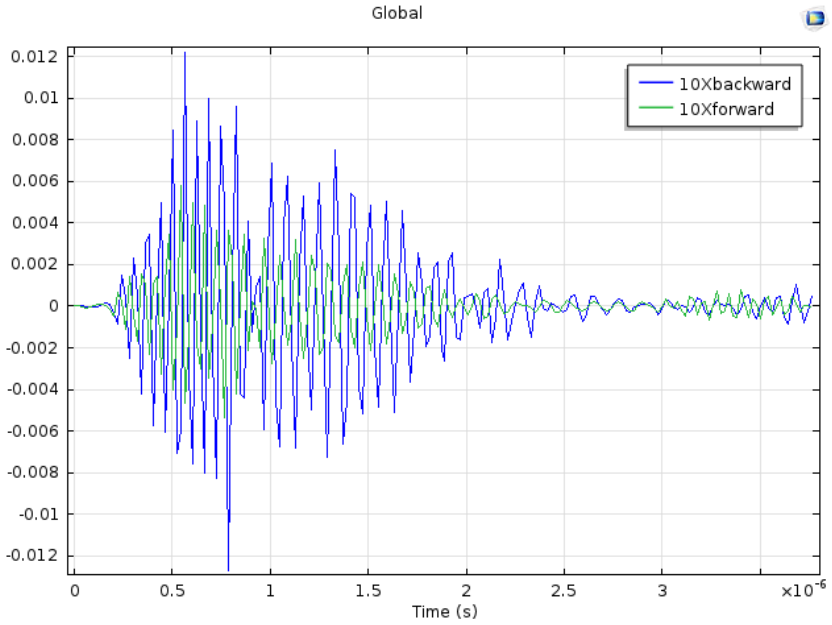

(b)

Figure 4.23 Substrate thickness is 150 microns a) 2D simulatiıon result b) signaloutput.

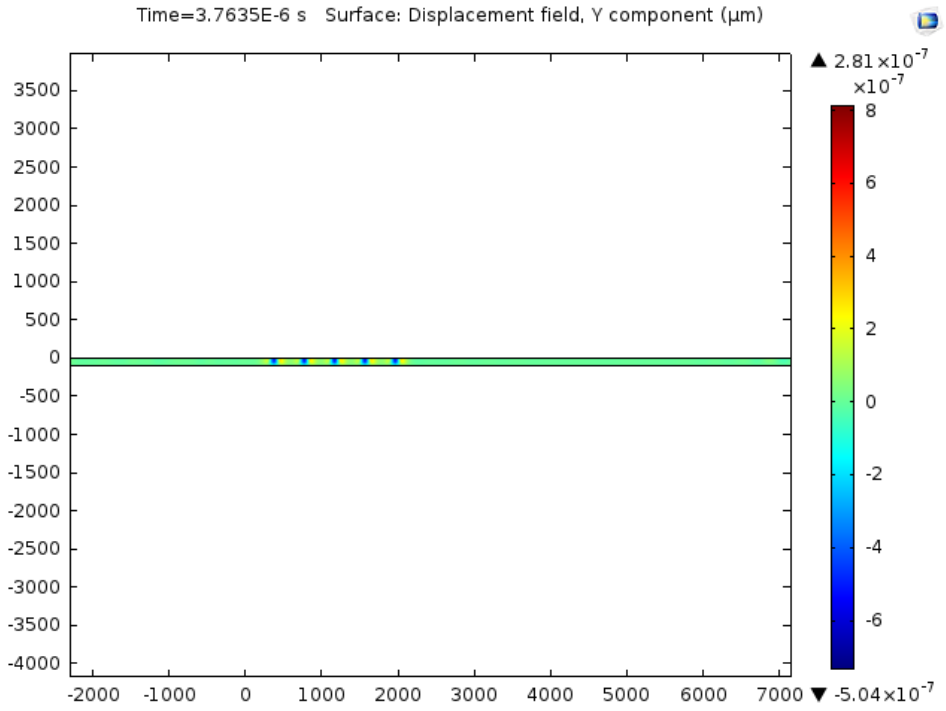

(a)

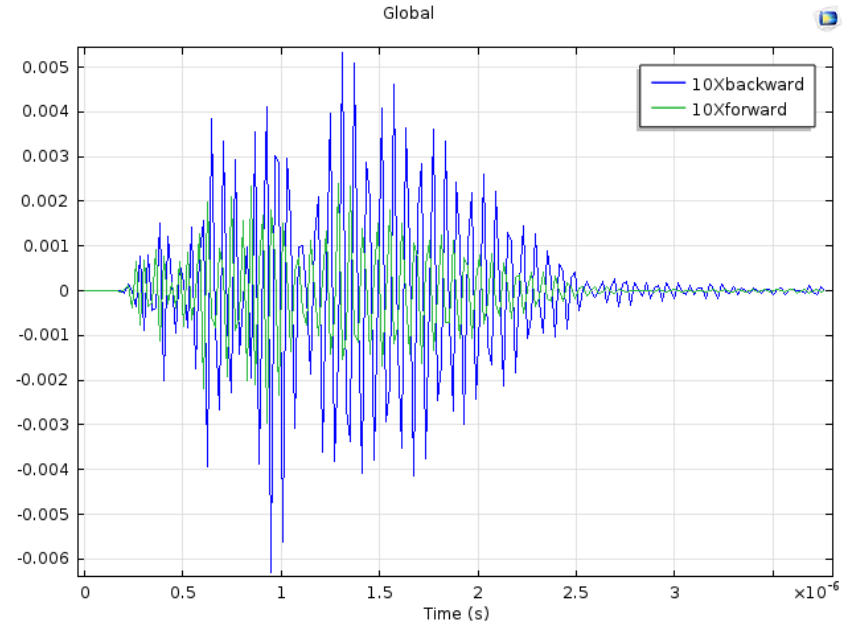

(b)

Figure 4.24 Substrate thickness is 100 microns a) 2D simulatiıon result b) signaloutput.

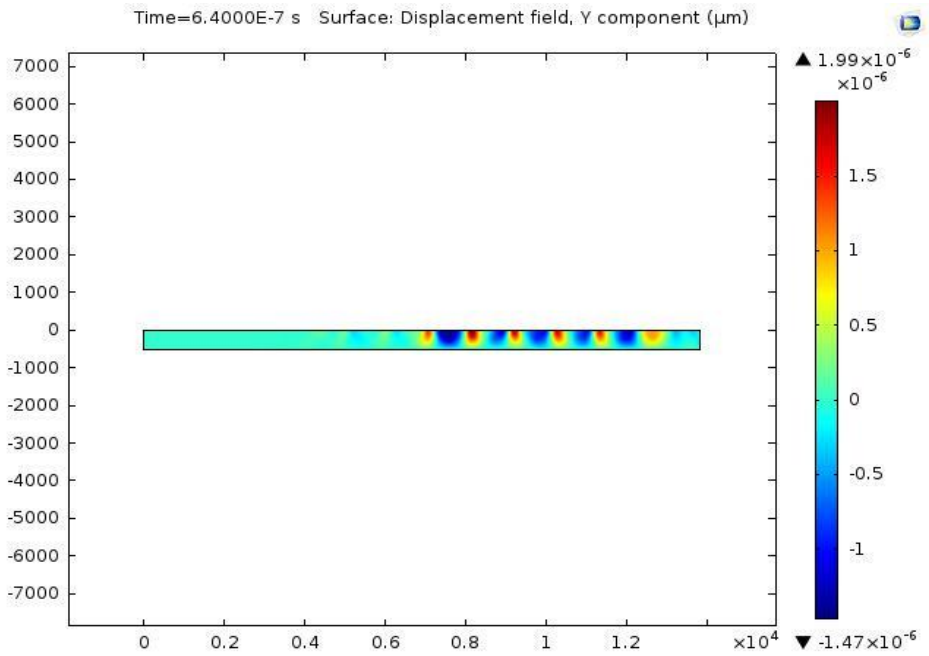
Time=6.4000E-7 s Surface: Displacement field, Y component (μm)
7000
6000
5000
4000
3000
2000
1000
0
-1000
-2000
-3000
-4000
-5000
-6000
-7000
0
0.2
0.4
0.6
0.8
1
1.2
×10^4
▲ 1.99×10^-6
×10^-6
1.5
1
0.5
0
-0.5
-1
▼ -1.47×10^-6

(a)

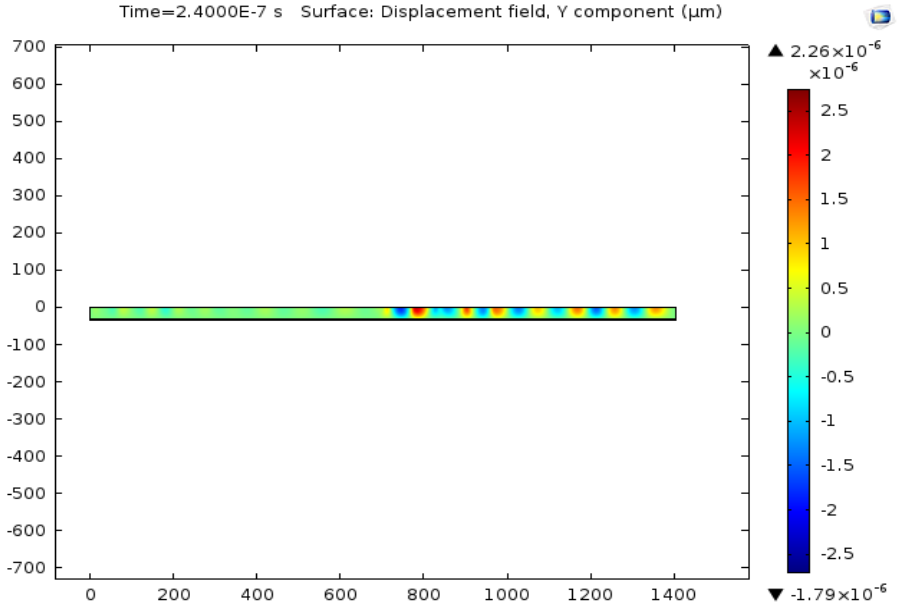
Time=2.4000E-7 s Surface: Displacement field, Y component (μm)
700
600
500
400
300
200
100
0
-100
-200
-300
-400
-500
-600
-700
0
200
400
600
800
1000
1200
1400
▲ 2.26×10^-6
×10^-6
2.5
2
1.5
1
0.5
0
-0.5
-1
-1.5
-2
-2.5
▼ -1.79×10^-6

(b)

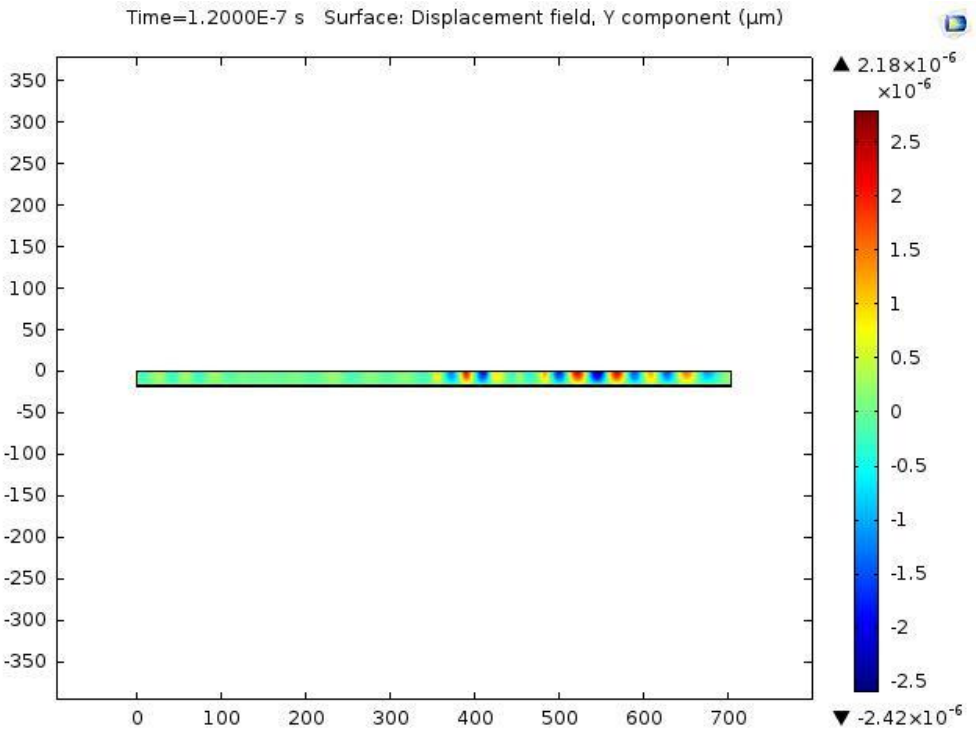

(c)

Figure 4.25 Substrate thickness is λ/2 (a) 3 MHZ device where λ is about 1052.7 microns (b) 50 MHZ device where λ is about 60 microns (c) 100 MHZ device where λ is about 31 microns.

Figure 4.25 proofs that our assumption about of relation of thickness of piezoelectric substrate to the directionality of surface acoustic wave is true. So, we decided to fabricate 7.5 MHz UDT IDT SAW. Where λ is 421 microns, delay is 3 mm and distance from wall also 3 mm.

Last step was to design and check 3D model of 3-port UDT IDT SAW. Because it was assumed in 2D simulation the width of IDT was going to infinity. However in real it is not. And it creates some harmonics that will effect on directionality of device.

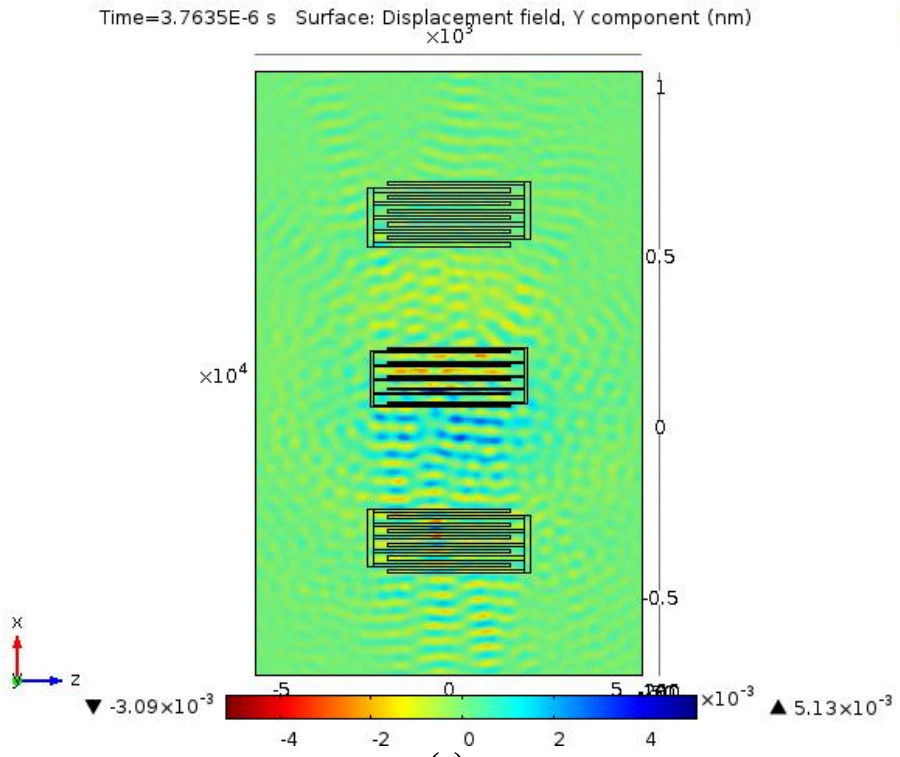

(a)

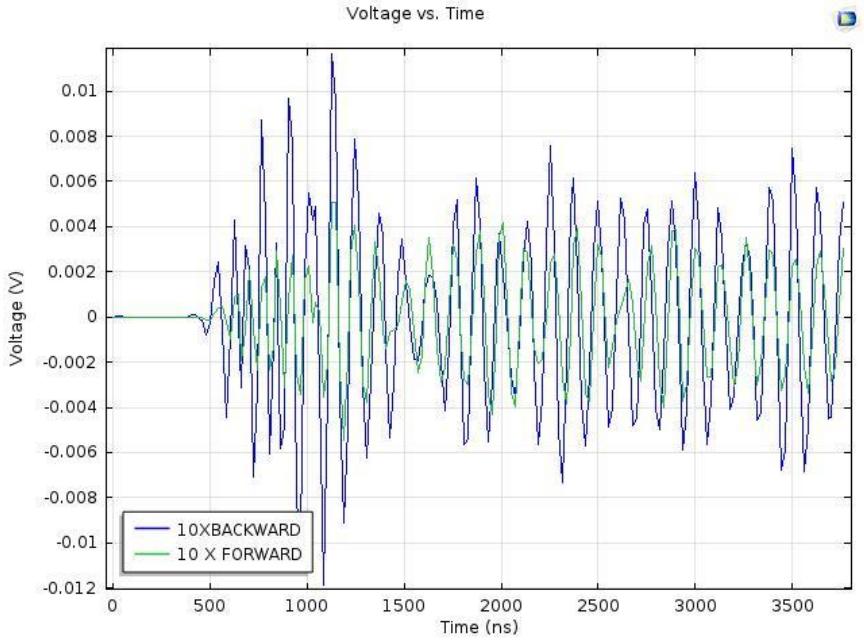

(b)

Figure 4.26 IDT width is 10λ where overlap of neighboring electrodes is 9λ a) 3D simulation reslut b) output signal.

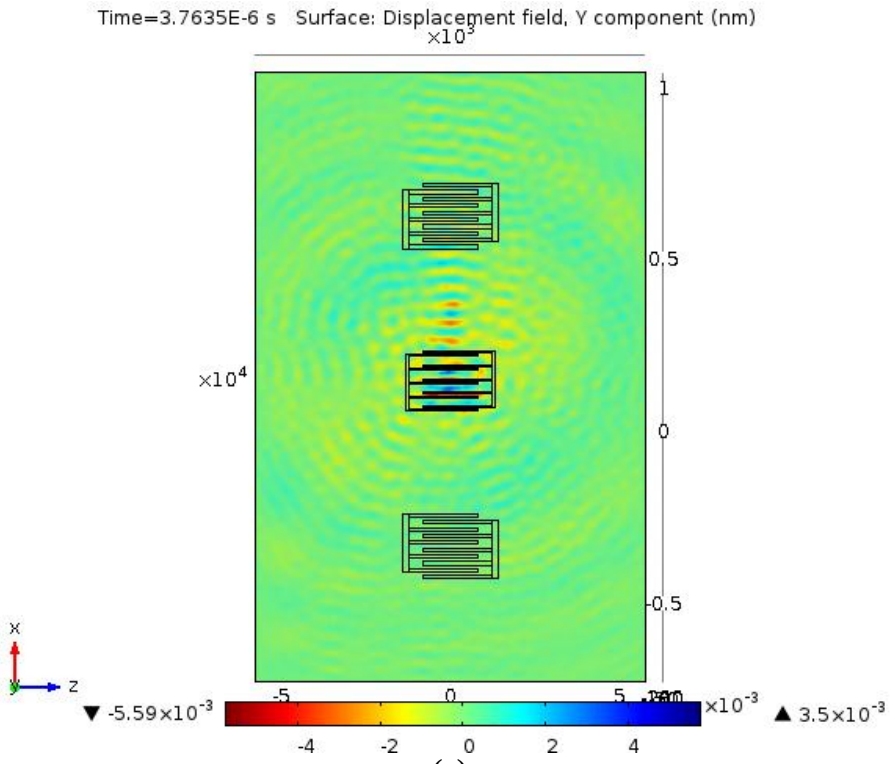

(a)

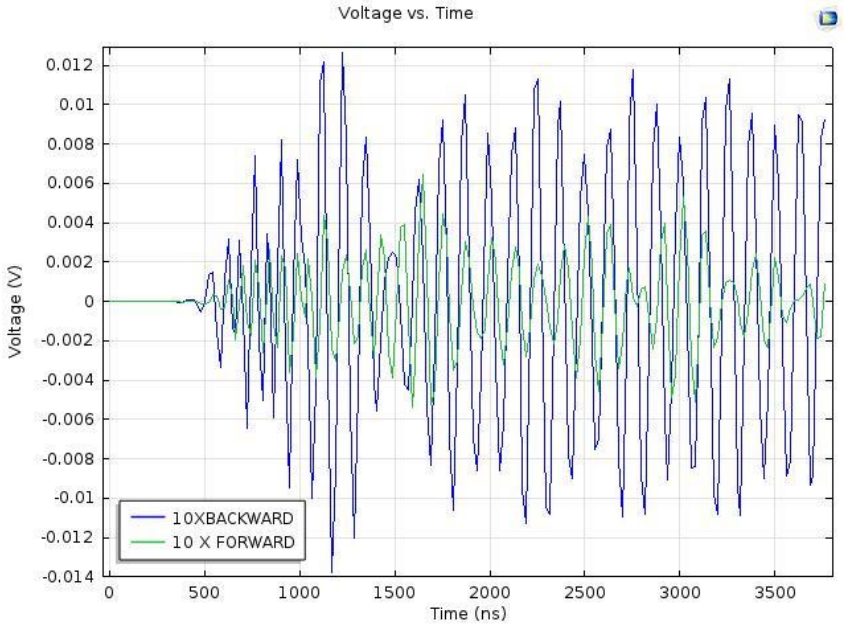

(b)

Figure 4.27 IDT width is 5λ where overlap of neighboring electrodes is 4λ a) 3D simulation reslut b) output signal.

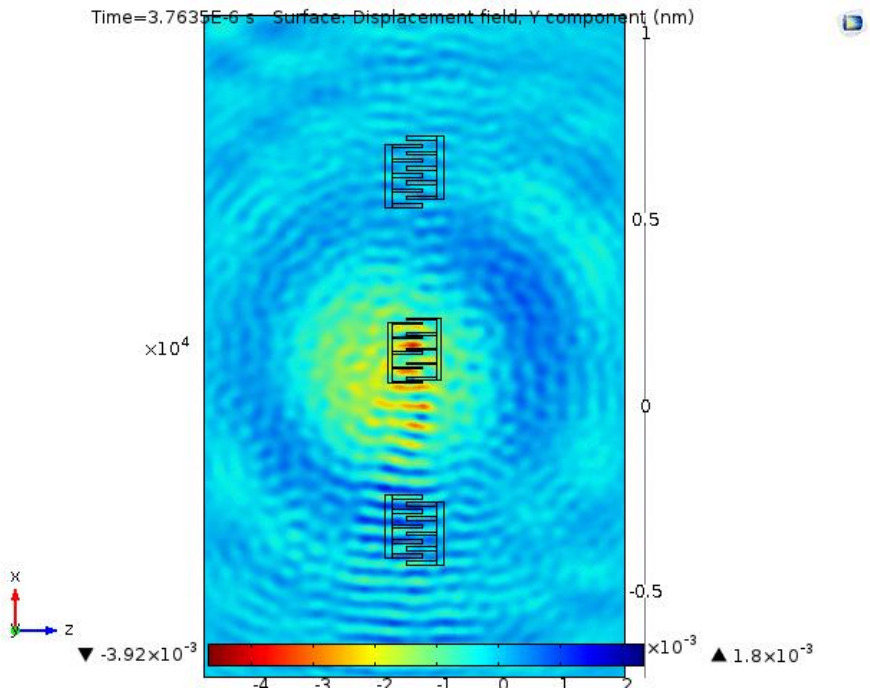

(a)

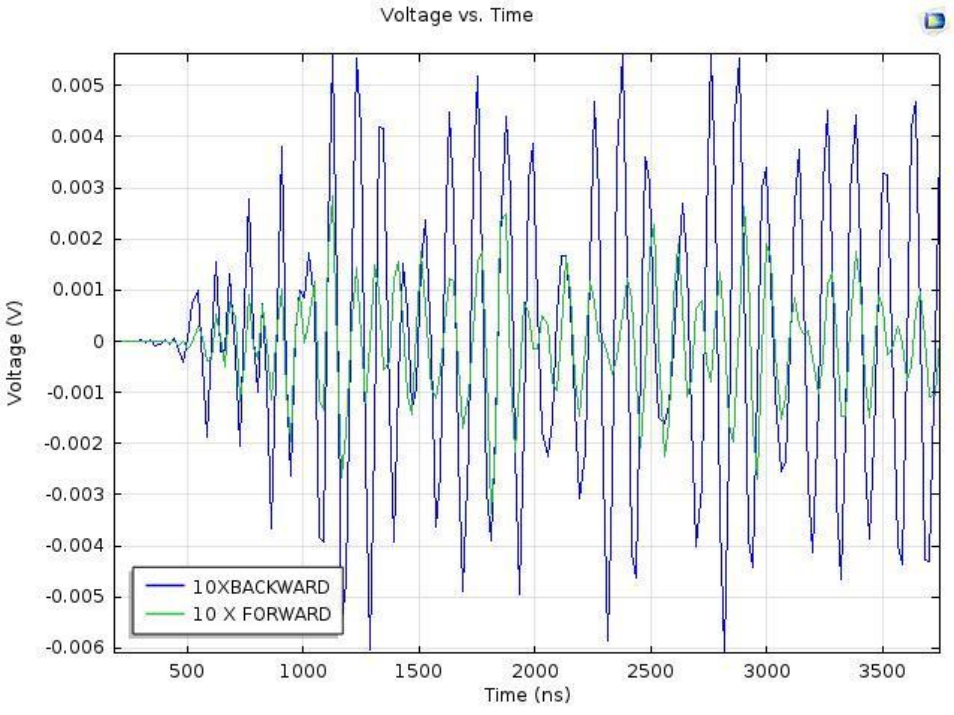

(b)

Figure 4.28 IDT width is 2λ where overlap of neighboring electrodes is 1λ a) 3D simulation reslut b) output signal

CHAPTER 5

FABRICATION OF 3-PORT UDT IDT SAW

5.1 PIEZOELECTRIC MATERIALS

Piezoelectric materials can be natural or man-made. The most well-known natural piezoelectric material is quartz, yet man-made piezoelectric materials are more effective and generally earthenware production. Because of their complex crystalline structure, the procedure with which they are made is extremely exact and needs to take after particular steps.

Quartz is well known piezoelectric material, but there are plenty of types of quartz. They can be categorized according to crystal cut or growing method e.t.c

-Quartz(SiO_2): One of the most used piezoelectric of nowadays industry. This quartz shows strong piezoelectricity due to its crystal orientation and are not too expensive in cost.

-Berlinite($AlPO_4$) Another type of piezoelectric material rarely used in industry.

-Gallium orthophosphate ($GaPO_4$): This type of piezoelectric material is almost same as quartz one because of their crystalline structure. But unlikely quartz, gallium orthophosphate's piezoelectric performance is twice better. That's why these type of piezoelectric materials mostly used in mechanical applications.

-Tourmaline this crystal can be in different colors like :black, green, violet and pink..

-Barium Titanate ($BaTiO_3$): Known also as electrical ceramics, it is usually replaced lead zirconate titanate *(PZT*) for piezoelectricity. It is used for microphones and transducers.

-Lead Zirconate Titanate (*PZT*): It is considered today one of the most economical piezoelectric element, hence it is used in a lot of applications.

-Zinc oxide (*ZnO*)

-Aluminum Nitride (*AlN*)

-Polyvinylidene Fluoride (*PVDF*) [10].

5.1.1 Quartz

After feldspar, quartz is the most copious mineral in the Earth's mainland outside layer, it is comprised of a ceaseless system of SiO4 silicon–oxygen tetrahedra, with between two tetrahedral every oxygen being shared, giving a general recipe Si02.

When mechanical stress is applied to a quartz an electricity is produced which state for the law of having piezoelectric property. Phonograph pickups were the first use of piezoelectric properties of quartz. Crystal oscillator is well known application of quartz in industry. Mineral also used while making quartz clock. Mechanical load applied to crystal oscillator device changes the resonant frequency, since this setting can be used to make very accurate measurements according to change in mass of crystal microbalance in a micro devices which are very small [11].

Quartz also varies according to their crystal orientation or crystal cut while manufacturing. Type of crystal orientation changes the properties of quartz. Because of in our lab we already have quartz we will use ST-quartz.

Table 5.1 ST-quartz properties

no.	material name	chinese	type	origin	crystal structure	Q-factor Q, ×10³
23	synthetic crystal quartz	水晶	synthetic crystal quartz	China	trigonalspace group 3M	300

Temperature frequency coefficient, TFC, ×10-6/°C	Dielectric constants: ε11/ε0, ε33/ε0	Piezoelectric constants: e11, e14	Resistivity
0.5	ε11=4.423 / ε33,=4.635	d33=2.1x10(-12)C/N, d11=+/-2.31x10(-12) ,d14=+/-0.73x10(-12)	20*1013ohm·m perpendicular to Z axis

Bulk Modulus	Rigidity Modulus(shear)	Young's Modulus	Coefficient of Thermal Expansion
36.4GPa	31.14GPa	97.2 (parallel to axis Z) 76.5 (perpendicular to axis Z)	7.1 ð 10-6 (parallel to axis Z) 13.2 ð 10-6 (perpendicular to axis Z) Ñ, °C-1

Thermal Conductivity	Velocity of Sound/Compression Wave	Chemical Stability (except hydrofluoric)	frequency const. of AT and Hi-k [kHz mm]	coupling coefficient of AT and Hi-k [%]
W/(m x K) (T = 25°C),10.7 (parallel to axis Z) 6.2 (perpendicular to axis Z)	ST 3158m/sec	insoluble in water	1660	8.8

Density(g/cm3)	Curie temperature	melting point (C)	Strain Point	Transformation Temperature (Tg)	Hardness
2.65	573	1467	573° C	573° C	Mohs:7

Elastic constants: c11, c33, c12, c13, c14, c44, c66	Transmission Range (Medium transmission ratio)	purity	Melting Method
C11=87 C12=7 C44=58 C13=13 C14=18 C33=106 C66 40	λ = 150 nm, ⩾0.80	SIO2 (99.96%)	Synthetic Hydrothermal method

As we already have shown in Table 6.1, we need only one parameter from table 5.1, velocity of sound. Which can change design parameters from equation $\lambda = {}^{c}/_{f}$. Where λ is desired wavelength, c is the speed of sound and f is target frequency of device. And as material type for IDT's we used titanium gold. The reason of using titanium gold is that, we already knew some parameter of titanium gold and helped us to easily fabricate 200 nm height IDT's

5.2 FABRICATION

In our university we have nano-technology lab. In nano-technology lab there is cleanroom where device of micro or nano size can be fabricated. Cleanroom is needed for avoiding dust and other not visible to human particles from fabrication process. Because dust or even very tiny particles can damage fabrication process and all process should be repeated. That's why while working in clean room there are rules should be obeyed, for example special type of wearing should be weared to avoid dust and other small particles. During fabrication different type of machines were used, which are: photolithography, reactive ion etching machine, and DC sputtering machine.

Photolithography, likewise termed optical lithography or UV lithography, is a procedure utilized as a part of microfabrication to example parts of a thin film or the majority of asubstrate. It uses light to exchange a geometric example from a photomask to a light-delicate synthetic "photoresist", or just "oppose," on the substrate. An arrangement of chemical medicines then either imprints the introduction design into, or empowers statement of another material in the craved example upon, the material

underneath the photograph stand up to. For instance, in complex coordinated circuits, a present day CMOS wafer will experience the photolithographic cycle up to 50 times. [12]

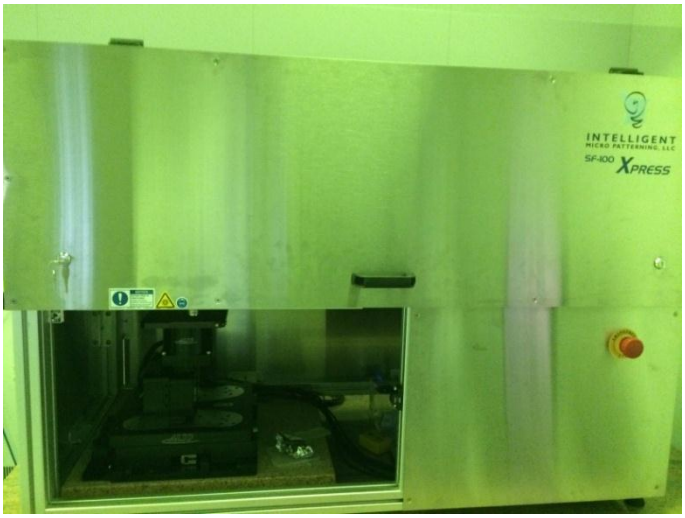

Figure 5.1 Photolithography machine in BINOTAM.

Reactive-ion etching (RIE) is a carving innovation utilized as a part of microfabrication. RIE is a sort of dry carving which has distinctive attributes than wet drawing. RIE utilizes chemically reactive plasma to evacuate material kept on wafers. The plasma is produced under low pressure (vacuum) by an electromagnetic field. High-vitality particles from the plasma assault the wafer surface and respond with it. Sputter is a physical vapor deposition (PVD) system for thin film deposition by sputtering. This includes launching material from an "objective" that is a source onto a "substrate, for example, a silicon wafer. Resputtering is re-emanation of the stored material amid the testimony handle by particle or molecule siege Sputtered particles shot out from the objective have a wide vitality appropriation, ordinarily up to many eV (100,000 K). The sputtered particles (normally just a little portion of the launched out particles are ionized on the request of 1%) can ballistically fly from the objective in straight lines and effect vivaciously on the substrates or vacuum chamber (creating resputtering).

Figure 5.2 RIE machine in BINOTAM.

Then again, at higher gas weights, the particles crash into the gas iotas that go about as a mediator and move diffusively, coming to the substrates or vacuum chamber divider and consolidating in the wake of experiencing an irregular walk. The whole range from high-vitality ballistic effect to low-vitality thermalized movement is open by changing the foundation gas weight. The sputtering gas is regularly an idle gas, for example, argon. For effective energy exchange, the nuclear weight of the sputtering gas ought to be near to the nuclear weight of the objective, so for sputtering light components neon is ideal, while for overwhelming components krypton or xenon are utilized. Receptive gasses can likewise be utilized to sputter mixes. The compound can be framed on the objective surface, in-flight or on the substrate relying upon the procedure parameters. The accessibility of numerous parameters that control sputter statement make it a perplexing procedure, additionally permit specialists a vast level of control over the

development and microstructure of the film. RIE sputter machine in our college is delineated in figure 5.3 [13]

Fabrication took 4 steps or 4 days. Each day about 1 hour was wasted. So, average fabrication time is about 5-6 hours.

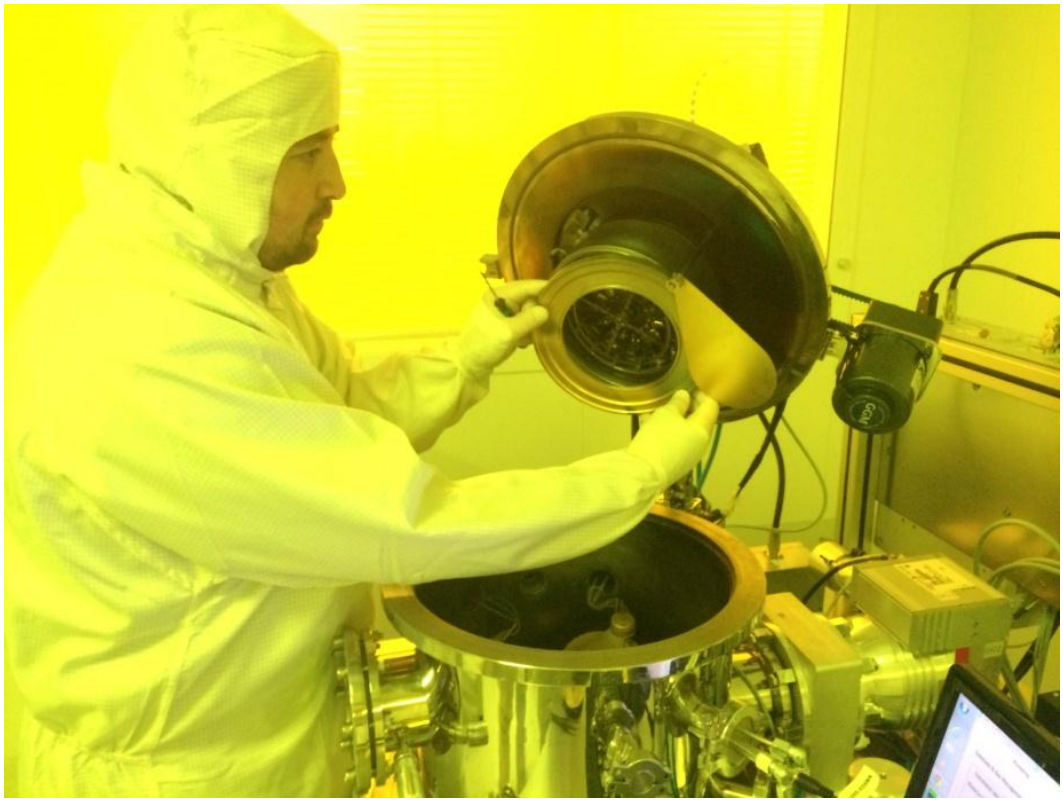

Figure 5.3 Sputter machine in BINOTAM.

In next figure, preparation of mask and fabrication of UDT IDT are shown step by step. For preparation of mask we are used chromium glass (also deposited and prepared in Faith University) and photoresist. For fabrication; titanium-gold alloy, photoresist and quartz.

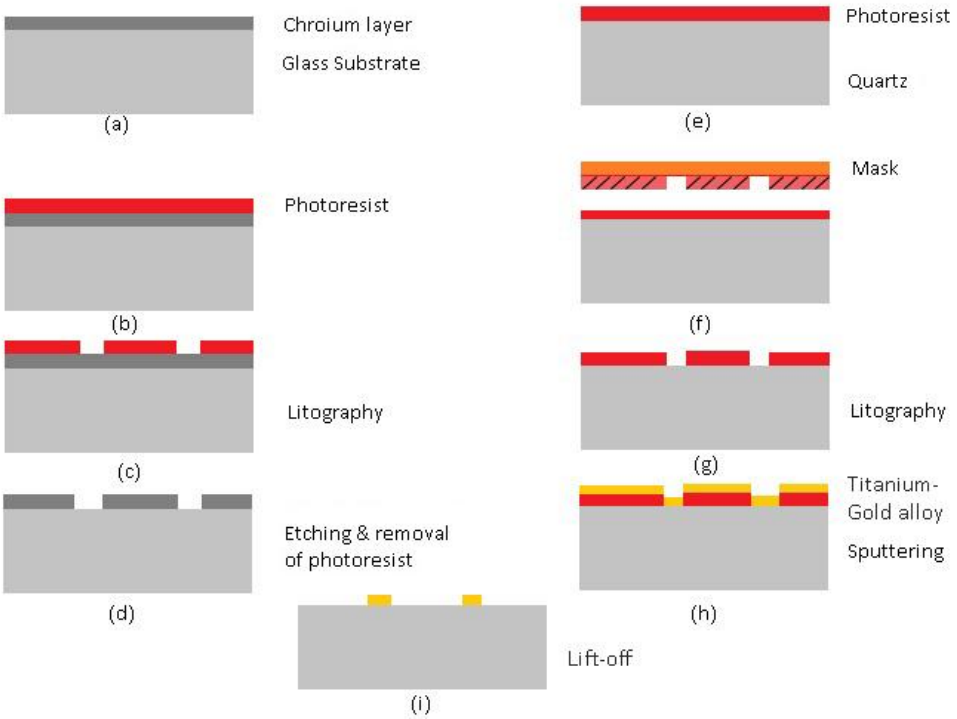

Figure 5.4 Fabrication steps of UDT IDT SAW devices.

CHAPTER 6

RESULTS AND DISCUSSION

In this thesis we wanted to achieve unidirectionality of surface acoustic waves that are generated on top of piezoelectric substrate. Hence, in table 6.1 shown optimal values of design parameters, which were selected after several simulations.

Table 6.1 optimal parameters for design

Parameters

Name	Expression	Value	Description
vR	3158[m/s]	3158 m/s	Rayleigh wave velocity
f0	7.5[MHz]	7.5000E6 Hz	Target frequency
lambda0	vR/f0	4.2107E-4 m	Target wavelength
w0	lambda0/8	5.2633E-5 m	Electrode width
h0	5*lambda0	0.0021053 m	Electrode length
gap_port	3*lambda0	0.0012632 m	Horizontal gap between p...
gap_term	lambda0	4.2107E-4 m	Vertical gap between term...
N0	5	5	Number of electrodes
pitch	lambda0	4.2107E-4 m	Pitch of electrodes
gap_vert	(N_cyc+2)*lambda0	0.0021053 m	Distance of electrode fro...
gap_horiz	(N_cyc+2)*lambda0	0.0021053 m	Distance of electrode fro...
t0	2*lambda0	8.4213E-4 m	Substrate thickness
N_cyc	3	3	Number of cycles to simu...
h_max	lambda0/5	8.4213E-5 m	Maximum mesh size
CFL	0.2	0.2	CFL number
tstep	CFL*h_max/vR	5.3333E-9 s	Maximum solver time step
V0	1.5[V]	1.5 V	Input voltage magnitude
eta0	0.001	0.001	Mechanical loss factor

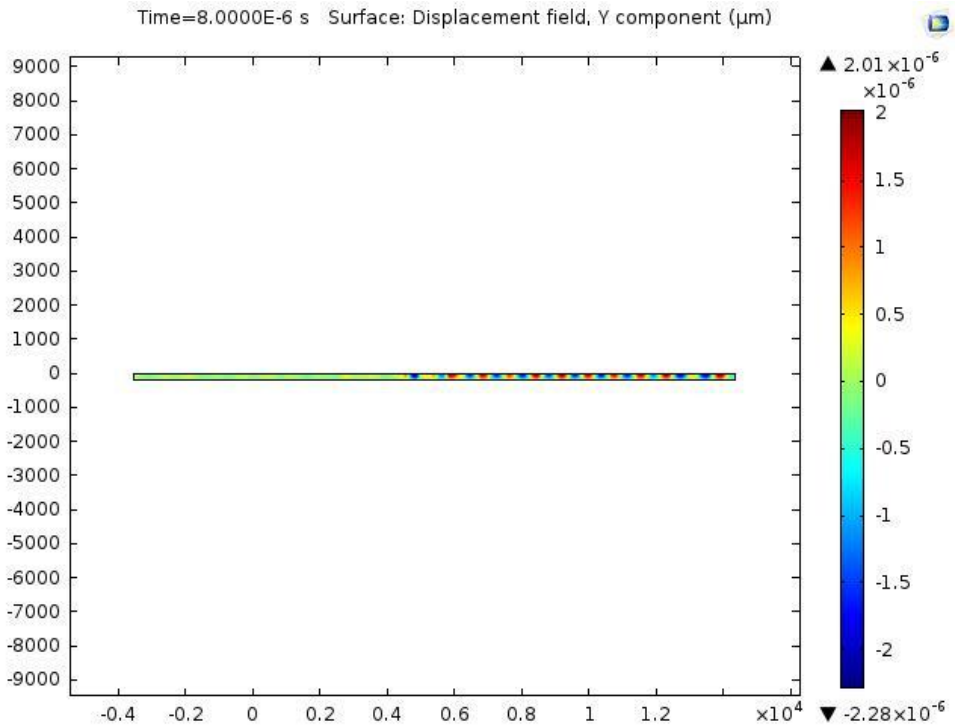

(a)

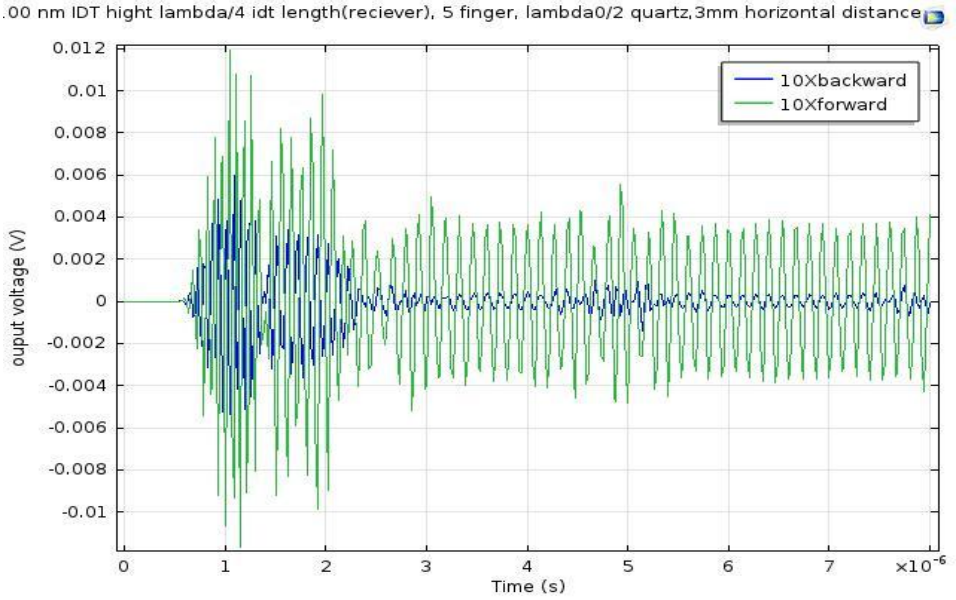

(b)

Figure 6.1 7.5 MHz SAW device simulation (a) image of SAW propagating unidirectional (b) Output signal.

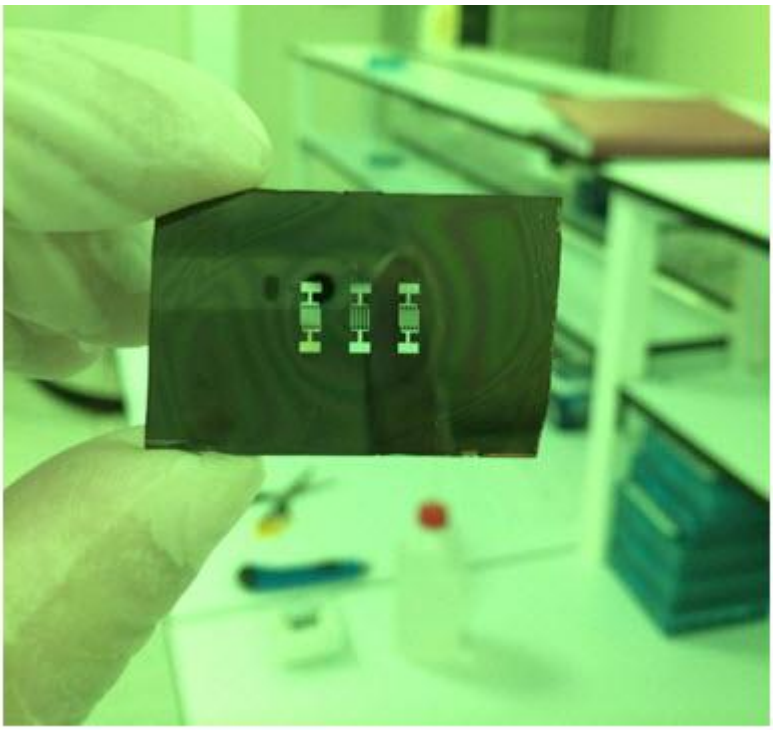

Figure 6.2 Fabricated mask of UDT IDT SAW device

From simulation result that is shown in figure 6.1 we can say surface acoustic wave is propagating only in one direction. Which proofs all mathematical concepts or we can say theory of unidirectioanlity that we were trying to explain,. And figure 6.2 is ready mask of UDT IDT SAW device, fabricated in Fatih university nano-technology lab cleanroom.

CHAPTER 7

CONCLUSION

During this research, not a few works were done. The goal was to generate unidirectional surface acoustic wave on top of a piezoelectric material. As we know, we cannot directly fabricate and do experiments and observations on a sample device. Firstly, it is not practical, secondly, can cost expensive and finally it can consume a lot time to get optimal design of device that can be capable of generating unidirectional surface acoustic waves. Hence, the first thing is to research the principles of generation of acoustic waves on top of piezoelectric substrate. In order to understand generation of acoustic waves at the surface of piezoelectric substrate, the idea of how piezoelectricity works should be examined. After, simulation and optimization via suitable software's should be done. All of works mentioned above were done during research.

To predict the performance of unidirectional surface acoustic interdigital transducer device, two software's were used to simulate two different cases. In first case the substrate was not exactly piezoelectric and membranes were made of cMUT(capacitevly micromachinned ultrasonic transducers) array. In this case silicon substrate was attached to fluid-half space. Assumption is that, device is surrounded by infinite liquid to demonstrate generation of acoustic waves inside of fluid. The reason to use infinite liquid boundary is to ignore some wave standings that we don't want. This method is very effective to create high unidirectional Scholte waves. Which can be very useful in bio-sensors. Simulations of this type device were via ANSYS software and the results were fabulous. Where, idea of separation and placement of cMUT arrays is as same as in second case.

In second case, substrate uses piezoelectric material and membranes are made of simple electrodes or Titanium Gold interdigital transducers. Electrodes are also placed

with arrangement of one four of desired wavelength as like as cMUT arrays. Simulation of this case was done via COMSOl multyphysics software. More than hundreds of simulations were done to achieve optimal parameters. Finally, best values were chosen after several parametric studies, to reach best performance. The simulation results were promising, which were shown in chapter 4.

The fabrication process is still in progress. We hope to see the same results as simulation ones. If we can fabricate UDT IDT 3-port device that is capable of generating highly directional waves, next thing will be to integrate this device with bio-sensors. I think, it can improve some of sensors that are currently being used in bio-medical areas.

REFERENCES

[1] *Surface Acoustic Wave Devices for Mobile and Wireless Communications*, Colin Campbell,(1998)

[2] G.S.Kino and R.S.Wagers, "*Theory of Interdigital Couples on Nonpiezoelectric Substrates*", Journal of Applied Physics, Vol. 44, (1973)

[3] J.C.Andle and J.F.Vetelino, "*Acoustic Wave Biosensors*", Proc. IEEE Ultrasonics Symposium,(1995)

[4] C.E.Bradley, J.M.Bustillo, and R.M. White, "*Flow Measurements in a Micromachined Flow System with Integrated Acoustic Pumping*", Proceedings of 1995 IEEE Ultrasonics Symposium,(1995)

[5] Auld B.A, *Acoustic fields and Waves in solids*, Willey: New York (1973)

[6] *Acoustic Wave Sensors: Theory, Design, & Physico-Chemical Applications* By D.S.Ballantine, Jr.,Robert M.White, S.J.Martin, Antonio.J.Ricco, E.T.Zellers, G.C.Frye, H.Wohltjen,(1996)

[7] Jeffrey.J.McLean, *Interdigital Capacitive Micromachinned Ultrasonic Trancducers For Microfluidic Applications*, (2004)

[8] K.Harhimoto, *Surfoce Acoustic Wave Devices in Telecommunications Modeling and Simulation*, Springer-Verlag, 2000

[9] Optimal Design of Three-IDT Type SAW Filter using Local Search Kiyoharu Tagawat , Kenji Tokunagat , Hiromasa Haneda', Tsutomu Igakit and Syunichi Sekit

[10] Antoine Ledoux, "*Theory Of Piezoelectric Materials And Their Applications In Civil Engineering*" (2011)

[11] Hale,D.R. (1948). "*The Laboratory Growing of Quartz*". Science 107 (2781)

[12] Jain,K. et al., "*Ultrafast deep-UV lithography with excimer lasers*", IEEE Electron Device Lett., Vol. EDL-3, 53 (1982)

[13] K.Ishii (1989). "*High-rate low kinetic energy gas-flow-sputtering system*". Journal of Vacuum Science and Technology A 7: 256–258